EVALUATION OF QUALITY OF APPLE SLICES DURING CONVECTION DRYING USING REAL-TIME IMAGE ANALYSIS

by

David Joseph Sampson

Submitted in partial fulfilment of the requirements
for the degree of Master of Science

at

Dalhousie University
Halifax, Nova Scotia

in co-operation with

Nova Scotia Agricultural College
Truro, Nova Scotia

August 2011

DALHOUSIE UNIVERSITY

NOVA SCOTIA AGRICULTURAL COLLEGE

The undersigned hereby certify that they have read and recommend to the Faculty of Graduate Studies for acceptance a thesis entitled "EVALUATION OF QUALITY OF APPLE SLICES DURING CONVECTION DRYING USING REAL-TIME IMAGE ANALYSIS" by David Joseph Sampson in partial fulfilment of the requirements for the degree of Master of Science.

Dated: August 26, 2011

Co-Supervisor: _____

Co-Supervisor: _____

Readers: _____

_____

DALHOUSIE UNIVERSITY

AND

NOVA SCOTIA AGRICULTURAL COLLEGE

DATE: August 26, 2011

AUTHOR: David Joseph Sampson

TITLE: EVALUATION OF QUALITY OF APPLE SLICES DURING CONVECTION DRYING USING REAL-TIME IMAGE ANALYSIS

DEPARTMENT OR SCHOOL: Department of Engineering

DEGREE: MSC CONVOCATION: October YEAR: 2011

_____

Signature of Author

Dedication

To my wife, Julia

You're an amazing friend
You've provided so much support
You kept my spirit so high
You've remained a pillar throughout my journey
And for that, I continue to owe you my life.

TABLE OF CONTENTS

LIST OF TABLES

LIST OF FIGURES

ABSTRACT

Computer-vision technology methods for assessing food quality were evaluated for their ability to provide non-contact measurements of apple slices. The methods evaluated were camera calibration, measurements of physical parameters of apple slices, and measurement of biochemical changes in apple slices. Each measure of food quality that was assessed by computer-vision was compared to a conventional method of measurement. The computer-vision system was capable of measuring area, thickness and volumes of apple slices. Color measurements from the computer-vision system were correlated with phenolic compound degradation in the beginning of the drying process and with hydroxymethylfurfural development later in the drying process.

LIST OF ABBREVIATIONS USED

SEM	Scanning Electron Microscope
CIE	Commission Internationale de l'Éclairage (International Commission on Illumination)
ASTM	American Society for Testing and Materials
RGB	Red-Green-Blue
HMF	Hydroxymethylfurfural
HPLC	High Performance Liquid Chromatography
UV	Ultra Violet
PPO	Polyphenoloxidase
MRP	Maillard Reaction Product
SIM	Selected Ion Monitoring
APCI	Atmospheric Pressure Chemical Ionization
SPE	Solid-Phase Extraction
MS	Mass Spectrometry
GC	Gas Chromatography
HSI	Hue-Saturation-Intensity
PNG	Portable Network Graphics
CAD	Computer Aided Drawing
a_w	Water Activity
X_0	Mono-layer water
X	Moisture Content
GLCM	Gray-Level Co-occurrence Matrix
VI	Virtual Instrument
BMP	BitMap
FRAP	Ferric Reducing Ability of Plasma
ORAC	Oxygen Radical Absorbance Capacity
ESI+	Positive Electron Spray Ionization
MRM	Multiple Reaction Monitoring
TPTZ	2, 4, 6-tris (2-pyridyl)-S-triazine
TE	Trolox Equivalents
$CaCl_2$	Calcium Chloride
cv	Cultivar

ACKNOWLEDGEMENTS

I send my sincerest thanks to my co-supervisors, Dr. H.P. Vasantha Rupasinghe and Dr. Qamar Zaman for their support, time, expertise, and use of their labs and equipment. Also a special thanks to Ajit Pal Kaur Joshi for her training, knowledge, and much needed assistance. Thanks to Dr. Bruce Rathgeber for his support on my committee and the use of the texture analysis equipment. Thanks to Dr. Young Ki Chang for your expertise and valuable insight for the image texture analysis.

Thanks to Scott Read for his expertise and talent in machining and metal work. Thanks to Theresa Osborne for listening and administrative advice. Thanks to the Tree Fruit Bioproduct research team for their support and training and occasional advice. Thanks to Dr. Alex Martynenko for obtaining the image analysis equipment and development platforms and getting me started.

I also acknowledge the Nova Scotia Department of Agriculture Technology Development fund, Noggins Corner Farm Ltd. and the Atlantic Canada Opportunities Agency for the generous funding they provided.

CHAPTER 1 INTRODUCTION

1.1 THERMAL PROCESSING OF FRUIT AND FOOD QUALITY

Thermal processing is a commonly used method of processing value-added dehydrated fruit snack products. The goals of thermal processing systems for food products are to: (i) destroy undesirable microorganisms; (ii) deactivate native enzymes which can compromise food quality; and (iii) create desirable quality characteristics, such as crispness and color (Marks 2006). Food quality is the combination of taste, smell, appearance, and texture. To assess food quality, disruptive contact measurements can be taken, which can cause food contamination and/or destruction. Since human perception is not consistent, these measurements are often subjective. The goal of this study was to use computer-vision to assess the quality of apple slices during the drying process as a non-destructive quality assessment method.

1.2 COMPUTER-VISION TECHNOLOGY IN THE FOOD INDUSTRY

The use of computer-vision technology has rapidly increased in development in the fields of quality inspection, classification, and evaluation in a large amount of food products (Sun 2004). Examples include bakery products, grain, vegetables, fruit, meat and many other food products have had computer vision systems developed (Sun 2004). Given a digital camera's spatial resolution, many features such as surface area, distance, shape, texture patterns, and color can be measured within a single image. The need for enhancements of computer-vision for food quality inspection has been assessed and successfully implemented within the food industry (Brosnan and Sun 2004).

To develop a real-time inspection system for apple slices, computer-vision must be studied to establish methods of measurement and implementation. Computer-vision systems have been used successfully in the evaluation of shrinkage, color and texture of apple slices during the drying process (Fernández et al. 2005). Computer-vision has also been used for the detection of surface blemishes of apples (Blasco et al. 2003). It is the intention of this research to design a computer-vision system for monitoring food quality during the drying process, review computer-vision techniques which can be used specific to apples, as well as study drying using real-time measurements of mass and images.

CHAPTER 2 LITERATURE REVIEW

2.1 COMPUTER-VISION AND FOOD QUALITY

Texture, flavor, appearance and color have been defined as major parameters of food quality (Abbott et al. 2004). Consumers use a combination or all of these food quality parameters to evaluate food before purchasing or consuming (Abbott et al. 2004). Computer-vision and image analysis has created many opportunities for measurements of spatial, colorimetric and textural features of various foods, including apple slices (Fernández et al. 2005; Blasco et al. 2003). Using segmentation techniques, such as thresholding and edge detection, image attributes can be extracted (Russ 1992). The scope of this research covers imaging of food quality indicators such as texture, shrinkage and color as well as factors which contribute to these parameters, such as moisture content, water activity, and polyphenolic compounds. Antioxidant capacity will also be assessed.

2.2 THREE-DIMENSIONAL (3-D) IMAGING OF BULK VOLUME

Bulk (geometric) volume is a directly measurable quantity, commonly used for the determination of shrinkage, density and porosity and can be defined as the space occupied by particles and the voids within the material (Webb 2001). To quantify bulk volume, many manual techniques have been developed based on liquid displacement such as pycnometry and buoyancy methods (Lozano et al. 1980; American Society for Testing and Materials 2004a). When periodic sampling is required, the procedure for measuring the volume becomes burdensome.

Image analysis has created many opportunities for bulk volume measurements due to its non-contact and non-destructive nature (Gunasekaran 2000; Mittal 1996).

Imaging of food quality is essential in avoiding contamination and destruction of food items (Lu and Sun 2000). Image analysis can provide more precise food quality measurements without extensive labour or other issues with human inspection (Pereira et al. 2009). Imaging of food quality may also exist in non-visible spectrums such as near-infrared, infrared, and ultraviolet spectrums. Image analysis can facilitate measurements in these ranges (Pereira et al. 2009).

There are many imaging techniques for the estimation of bulk volume of regularly-shaped objects with single camera (Levine et al. 1990; Deltel, et al. 2001; Fernández et al. 2005; Martynenko 2006). However, imaging of bulk volume of irregularly-shaped objects require either computed tomography (Lee et al. 2006; Pintavirooj and Sangworasil 2002), or laser light projection (Lee 2002), or stereoscopic imaging (Ruff et al. 1995; Nishino et al. 2000). The cost and processing resources of computed tomography make the feasibility of using such technology limited (Russ 2005). Preliminary studies have shown that stereo imaging can be used for the measurement of bulk volume of three-dimensional objects, particularly apple slices.

2.3 Texture Measurements

Texture is defined as a sensory property detected by humans using the sense of touch. It is a multi-parameter attribute described by an array of characteristics related to the structure of the sample (Szczesniak 2002). Szczesniak (2002) defines a number of primary and secondary properties. Cohesiveness is a primary property describing the extent to which a sample can be deformed before it ruptures. Fracturability is a secondary property and is defined as the peak force required for a sample to break. Research has shown that crispness is a desirable characteristic in snack foods (Fillion and

Kilcast 2002; Roudaut et al. 2002; Joshi et al. 2007). It is important particularly for industries wishing to develop texturally attractive foods to understand relationships between food texture perception and food structure (Wilkinson et al. 2000). It has been shown in fried tortilla chips that an increase in porosity results in an increase in crispness (Kawas and Moreira 2001).

Instrumental and sensory approaches to quantifying crispness and texture have been reviewed (Roudaut et al. 2002). Puncture tests using a texture analyzer have been performed to evaluate the crispness of potato chips (Pedreschi et al. 2006; Garayo and Moreira 2002) with the overall finding that crispness was a function of water activity (Katz and Labuza 1981). Mechanical analyses of crackers have indicated that the initial slope of a force-deformation curve is a good indicator for the evaluation of crispness. Fracturability, mechanical work, and cohesiveness were found to be significant indicators of crispness of popcorn (Katz and Labuza 1981). Mechanical analysis of potato chips did not produce useful information which could be used to evaluate crispness (Katz and Labuza 1981). Peak force, area under the curve and initial slope measurements of dried apple slices are informative and can be an indicator of crispness.

2.4 Porosity Determination

Porosity can be defined as the ratio of the total volume of space within a porous structure to the total volume of the porous structure (Webb 2001). Porosity can be measured using a number of methods such as volume/density methods, water saturation methods, water evaporation methods, using a scanning electron microscope (SEM) as well as from using shrinkage and moisture measurements using analytical correlations (Webb 2001).

Analytical correlations based on volume and moisture content have been successfully used to determine the porosity of ginseng during the drying process (Martynenko 2008).

2.5 Water Activity

Water can affect the safety and stability of stored food products. High water activities can promote the growth of pathogens and other microbial organisms (Vos and Labuza 1974). There are essentially no physical factors of food products that are not affected by water (Lewicki, 2004). Water activity can be determined using a correlation of water activity as a function of moisture content and temperature (Thompson 1972). Crispness intensity as a function of water activity was evaluated for popcorn as well as moisture as a function of water activity for popcorn, puffed corn curls, saltine crackers and potato chips (Katz and Labuza 1981). Critical moisture conditions for textural acceptance by consumers are better to be evaluated by water activity instead of moisture measurements (Katz and Labuza 1981). Measurements outlined in Katz and Labuza's (1981) research has not been extended to apple slices. The information can be useful in determining optimum drying conditions from real-time measurements.

2.6 Color Measurements

Consumer perception of color is a very important quality parameter when selecting fruit and vegetables, as consumers will often not review the textural or flavor aspects when the color is found to be unacceptable (Francis 1995). Color is often represented as a combination of three values described in a three-dimensional color space. Because equal distances in other color spaces, such as XYZ and xyY, did not represent uniformly perceptible color changes, the Commission Internationale de l'Éclairage (CIE) developed the CIE L*a*b* color space in 1976 (CIE 2007).

Different color indices have been used to quantify color as a single value composed of three color measurement parameters. A common index used in food measurements is the whiteness index calculated with CIE L*a*b* (Judd 1963) and is calculated by the following equation:

$$WI = 100 - \sqrt{(100 - L^*)^2 + a^{*2} + b^{*2}} \quad (1)$$

Methods for calculating the whiteness or yellowness index have been defined by the American Society for Testing and Materials in ASTM E313 (American Society for Testing and Materials 2004b). Color measurements represented as red-green-blue (RGB) have been extracted from digital images and successfully converted to the CIE L*a*b* color space (León et al. 2006). Computer vision systems have been developed to measure the color of potato chips (Mendoza et al. 2007; Segnini et al. 1999a; Segnini et al. 1999b; Pedreschi et al. 2006).

2.7 Enzymatic Browning

Polyphenolic compounds are plant secondary metabolites, some of which have beneficial antioxidant properties (Joseph et al. 2005). Flavonoids are a particular class of polyphenolic compounds which have many roles within the plant. Research has shown that a number of flavonoid sub-classes have antioxidant and biological properties, such as proanthocyanidins in red wine and flavonols extracted from Ginkgo leaves used to treat symptoms of Alzheimer's Disease (Defeudis and Drieu 2000; Sato et al. 2001). For apples, the major flavonoid sub-classes which contribute to antioxidant activity are anthocyanin, catechins, flavonols, and dihydrochalcones, but their concentrations are cultivar dependant (Huber and Rupasinghe 2009). Many natural polyphenolic compounds are desirable, but 5-Hydroxymethylfurfural (HMF) that results from non-

enzymatic browning through the Maillard reaction is an exception to the rule. For this thesis, the relationship between antioxidant capacity and enzymatic browning as the result of the drying process was investigated.

Drying is used for removing moisture from food products to preserve them by lowering the moisture content and water activity to minimize microbial growth and enzymatic reactions (Chen 2008). However, high drying temperatures accelerate enzymatic browning compared to lower temperatures resulting in a loss of food quality and various effects on the total phenolic content depending on the type of food (Turkmen et al. 2005; Jamradloedluk et al. 2007). Therefore, there is a need to develop quality control methods through the use of a computer vision system. Such a process could be used by industry for indicating the end of drying for various food products.

2.8 Ferric Reducing Ability of Plasma

The ferric reducing ability of plasma (FRAP) assay measures the ability of a sample to reduce the reagent ferric-tripyridultriazine (TPTZ) to its ferrous form in a low pH environment. The absorbance change is linearly related to the antioxidant capacity of a sample (Benzie and Strain 1996). The FRAP assay has been used to assess the antioxidant capacity in many cultivars of apples (Tsao et al. 2005; Henríquez et al. 2010). In both studies, the FRAP assay was sensitive and correlated with total phenolic content.

2.9 Polyphenolic Compounds As Antioxidants

The first step of polyphenolic extraction for quantification using high performance liquid chromatography (HPLC) is to crush the raw sample tissue and add a solvent (Wang et al. 1996). The substrate is then filtered and placed in a sonication bath to facilitate extraction. The extract containing the polyphenolic compounds is filtered and quantified

by HPLC. Solvents used for extractions from fruit typically include acetone, ethanol, or methanol (Wang et al. 1996). HPLC separates the compounds based on hydrophilicity and detects them using the absorbance of visual or UV light. Mass spectrometry can also be used to identify and quantify specific compounds after HPLC separation and can provide verification of HPLC measurements.

2.10 Thermal Sensitivity of Polyphenolic Sub-classes

The drying temperature is important for determining the drying rate of food. The sensitivity of different sub-classes of polyphenolic compounds varies with respect to temperature (Madrau et al. 2009). Apricot samples dried at two temperatures (55 and 75 °C) were compared against fresh samples to determine the effect of drying on polyphenolic content and antioxidant activity (Madrau et al. 2009). Chlorogenic and neochlorogenic acid, catechin, epicatechin, rutin, and quercetin 3-*O*-glucoside were evaluated, but only chlorogenic acid and neochlorogenic acid had a significant decrease following drying for the Cafona cultivar. However, the concentration of these compounds was significantly higher when dried at the higher temperature. Madrau et al. (2009) attributed this finding to polyphenol oxidase (PPO) activity as it takes longer to deactivate this enzyme at lower temperatures. There was also a significant decrease in the L* and a* values of the apricot pulp indicative of enzymatic browning (assuming apricots are initially orange in color). Overall, there was an increase in antioxidant activity dependent on temperature in the Cafona cultivar, but not in the Pelese cultivar. The increase in antioxidant activity with drying of apricots contradicted the findings for mulberry leaves dried at 40, 60, 70, 80, and 110 °C which resulted in decreased antioxidant activity (Katsube et al. 2009).

Polyphenolic compounds including selected anthocyanins were studied in plums (Piga et al. 2003). Two drying treatments were used; the first was 85 °C until the moisture content reached 50% then was adjusted to 70 °C for the remainder of the process and the second was at 60 °C for the entire duration. Hydroxycinnamic acids, anthocyanins, and flavonols were evaluated after each treatment. There was no significant change in chlorogenic acid or neochlorogenic acid when dried at the higher temperature, but there was a significant decrease in both at the lower temperature. In contrast, Raynal et al. (1989) found that there remained 27.1% and 36.5% of the chlorogenic and neochlorogenic acids respectively in plums (cv 'Agen'), when dried for 8 hours at 55 °C. There was also significant degradation in these acids regardless of temperature within the first two hours of drying (Raynal et al. 1989). PPO reactions may have more time to oxidize these compounds at the lower drying temperature. The anthocyanins were completely destroyed in the sugar plum variety after both drying treatments (Piga et al. 2003). In the President variety, traces of cyanidin 3-rutinoside and an equivalent form of cyanidin 3-rutinoside were still present. These traces were explained by the initially high levels of these compounds in the President variety of plums, provided their destruction followed a first order reaction which would result in instrumentally detectable anthocyanin levels. Since the Sugar variety had low initial levels of anthocyanins, the levels dropped below instrumental detection. Catechin was completely destroyed after drying at both temperatures indicative of PPO activity (Piga et al. 2003). In all other cases, there were significantly lower levels of flavonols when dried at the higher temperature indicating no direct relationship between the degradation of flavonols and polyphenol oxidase (Piga et al. 2003). Despite the degradation of some

polyphenolic compounds, the levels of antioxidant activity tended to be significantly higher with higher drying temperatures for the sugar variety. The President variety had a significant decrease in antioxidant activity at 60 °C, but a major increase when dried at 85 °C (Piga et al. 2003). The increase in antioxidant activity with increasing temperature can be explained by the development of hydroxymethylfural (HMF) which is a product of the Maillard reaction. However, the increase in HMF at 60 °C in the President cultivar was not enough to compensate for the loss of phenolic compounds suggesting HMF has a higher antioxidant capacity than phenolic compounds (Piga et al. 2003).

Mulberry leaves were dried at 5 temperatures (40, 60, 70, 80, 110 °C) and freeze dried (Katsube et al. 2009). Phenolic content significantly decreased at a drying temperature of 70 °C, whereas above 70 °C there was a slight increase. This finding differs from the findings of Madrau et al. (2009) and Piga et al. (2003) which indicated a significant decrease at 55 and 60 °C, particularly for chlorogenic acid and rutin possibly because of a shorter drying time. Antioxidant activity in the mulberry leaves was directly related to the decrease in polyphenolic compounds and increase in drying temperature which was not typical of previous findings for apricots and plums (Madrau et al. 2009; Piga et al. 2003).

Antioxidant activity of red grape pomace peels was not significantly different at 60 °C than that of freeze dried peels, but was significantly lower at 100 and 140 °C accompanied by a reduction in total extractable polyphenols (Larrauri et al. 1997). Therefore, in this thesis study, it was necessary to determine drying temperatures which promoted optimal antioxidant levels.

2.11 Preferred Substrate For Polyphenol Oxidase

Polyphenol oxidase (PPO) is located in the chloroplast and mitochondrial fractions of cells in both the apple peel and flesh (Harel et al. 1964). The activity of this enzyme was found to be optimal at a pH of 5.1 and 7.3 (Harel et al. 1964). Mitochondrial activity was the same at both pH values, while the chloroplast PPO was more active at a pH of 5.1 (Harel et al. 1964). Chlorogenic acid was determined to have a high substrate specificity for polyphenol oxidase, while epicatechin had a specificity of approximately 54%, catechol 41%, and o-hydroxycinnamic acids were not oxidized at all compared to 4-methylcatechol (Harel et al. 1964). As chlorogenic acid is also the preferred substrate for PPO in apple tissue, it was one of the main phenolic compounds of interest in this thesis study.

2.12 HMF/Non Enzymatic Browning

Maillard reactions serve many purposes in food processing and storage, such as enhancing the appearance and aromas of food, as well as improving textural characteristics (Teixidó et al. 2008). These reactions are triggered during the heat treatment of foods containing reducing sugars and amino acids. The first intermediate compounds formed from Maillard reactions are Amadori compounds which are precursors to many of the final Maillard reaction products (MRPs) (Sanz et al. 2001). Much research has been conducted in these reactions because of their antioxidant properties, but also their possible toxic properties, particularly found with the compound HMF (Ulbricht et al. 1984). Identifying and understanding these compounds would aid in optimizing food processes with respect to Maillard reactions.

HMF is a common MRP and is one of the decomposition products of ascorbic acid. HMF was discovered in prunes dried at temperatures between 60 and 85°C, and was also shown to have antioxidant properties (Piga et al. 2003). A similar observation was made for apricots (Madrau et al. 2009). HMF has been found to be mutagenic and possibly carcinogenic despite its antioxidant properties (Omura et al. 1983). HMF is a good indicator of inadequate storage time or temperature and has been used for jams and infant foods (Rada-Mendoza et al. 2004). HMF also contributes to color, flavor, and texture of bread, cereals and hazelnuts (Teixidó et al. 2008). The most common method for measuring HMF is with HPLC using UV detection at 280 nm (AOAC method 980.23). The problem with this method is that many other compounds can be detected thereby distorting the measurement of HMF. Mass spectrometry has been shown to accurately identify and quantify HMF in fruit and fruit based foods and many other food products (Teixidó et al. 2006; Teixidó et al. 2008; Gökman and Şenyuva 2006).

2.13 Mass Spectrometry Methods For HMF Quantification

A primary application of mass spectrometry techniques in commercial sectors of food production is quality control. Mass spectrometry has the potential to provide rapid, accurate, and unequivocal measurements of product degradation using MRPs. Since there are many natural compounds in foods which absorb light wavelengths at 280 nm using HPLC, mass spectrometry becomes a useful method to unambiguously identify HMF (Gökman and Şenyuva 2006). One study used mass spectrometry to measure the HMF content of baby food (Gökman and Şenyuva 2006). The mass spectrometer used an atmospheric pressure chemical ionization (APCI) source, and was set for selected ion monitoring (SIM). The mass to charge (m/z) ratio of the ions of interest were 109 and

127. Due to interference from other molecules, solid-phase extraction (SPE) cleanup was used to remove interfering compounds so that HMF could be adequately concentrated. The purity of the measurement was verified by looking at the ratio between the two peaks (m/z 127:m/z 109 = 1.12). Prepared samples of baby food were tested to ensure the method was accurate. The recovery rate for HMF from these known samples was greater than 90%. This method was also used to measure the HMF levels in other baby foods, one of which had a concentration of 57.18 μg/g HMF. It was concluded that using an SPE cleanup could effectively enhance the accuracy of the assay and could be done in under 20 minutes (Gökman and Şenyuva 2006).

A similar study was conducted to determine the HMF content in honey, breakfast cereals, orange juice, biscuits and jam using gas chromatography (GC) couples with mass spectrometry (GC-MS) (Teixidó et al. 2006). The MS used a positive electron ionization technique and acquired data using a full scan over the range m/z 40-200 with 0.66 s per scan. SPE cleanup was employed as well. An HMF derivative (Furan-3-etinil-trimethylsilane) was used as the standard which was added to Milli-Q water. This compound exhibited similar chromatographic behavior and chemical properties and was not contained in the food. The HMF derivative was detected at m/z 198, though this peak was small. The ion with m/z 183 (M – CH3) was selected for quantification of HMF. The food sample concentrations of HMF covered a range, but typically matched what was previously reported in literature. The experiment showed that SPE cleanup was also effective at enhancing GC-MS measurements with the total procedure taking approximately 30 minutes (Teixidó et al. 2006).

A further enhancement to the previously mentioned procedure consisted of liquid chromatography in combination with multi-stage tandem mass spectrometry (HPLC-MS-MS) used to analyze HMF in honey, breakfast cereals, orange juice, biscuits and jam (Teixidó et al. 2008). To obtain more structural information and to verify their findings from HPLC-MS-MS, MS3 (using an ion trap) was used. The ion m/z 81 was the only observed product ion which attributed to the loss of an aldehyde (M + H – H2O – CHO). The signal-to-noise ratio was similar between the MS-MS and MS3 methods, but the MS3 method was significantly more accurate than LC-UV methods and comparable to LC-MS operating in SIM mode. Therefore, LC-MS3 can accurately provide 4 inspection points including UV absorption at 280 nm, the presence of m/z 127, m/z 109, and m/z 81. When the HMF measurements in the food were compared to GC-MS, no significant differences were observed (Teixidó et al. 2008). It was concluded that tandem mass spectrometry could be adequately used instead of LC-UV analysis and that MS3 provided a good verification method for HMF (Teixidó et al. 2008). LC-MS-MS was used for this thesis because of no reported difference between the results of these methods.

Information concerning HMF is still limited and so it would be useful to determine the mass spectra of HMF in its pure form. Also, there are problems associated with the two main methods of calibrating MS with HMF. The first involves adding a known concentration of HMF to the baby food. However, if HMF is already present in the food the calibration curve would be offset. The second uses HMF derivatives that, in theory, react similarly in the mass spectrometer. However, this changes the interpretation of the results altogether, giving different m/z values. Therefore, one solution for the baby

food study would be to show the differences in the mass spectra before and after the addition of HMF.

CHAPTER 3 OBJECTIVES

The overall goal of this study is to understand possible uses of computer-vision to assess the food quality of apple slices during the convection drying process.

The specific objectives are as follows:

Objective 1: To objectively prepare the computer-vision cameras for measurements by (i) determining the specific camera settings such as black level, gain, and saturation which will optimize the lighting and color measurements, (ii) correct non-uniform illumination and spatial distortions, and (iii) determine the correlations between computer-vision measurements and physical measurements (area, thickness, color) using inert objects.

Objective 2: To assess the ability of the computer-vision system to measure volume and texture characteristics (peak force, initial slope and work done according to stress-strain curves) of the apple slices using the information collected from objective 1.

Objective 3: To determine if camera color measurements correlate with polyphenolic degradation and polymerization and to assess antioxidant capacity of apple slices after drying treatments at different temperatures.

In objective one, camera specific parameters were determined to produce an image with high contrast and color range. Lens characteristics were determined and spatial distortion was corrected. Illumination characteristics were determined and non-uniform illumination was corrected. Correlations between computer-vision measurements and physical measurements were found using inert objects.

In phase two, the correlations and non-contact measurement techniques developed in phase one will be used to make real-time measurements of apple slice quality during the drying process. Different drying conditions will be used to examine the robustness of

the correlations developed at different temperatures. Image texture patterns in relation to food texture characteristics were also explored.

Phase three investigated the degradation of polyphenolic compounds and antioxidant activity. The study looked at color changes measured with the computer-vision system in relation to the loss of polyphenolic compounds and antioxidant activity as well as examined the effects of Maillard reactions on apple slice quality during the drying process.

CHAPTER 4 PREPARING A CAMERA FOR COMPUTER-VISION USE

ABSTRACT

Comparing computer-vision measurements between systems can be a difficult task because of the differences in hardware and configuration of each system. Methods to assess the ability for the computer-vision system to measure geometric parameters such as area, thickness, and volume, and to measure color were tested to determine the suitability of using the computer-vision system for these measurements. Each method used an object that could easily be standardized or has already been standardized so that the measurements from the computer-vision system could be presented in common units while accounting for lens distortions and non-uniform illumination. The computer-vision system was capable of measuring surface area of flat objects with an accuracy of ±11.01 mm^2, and thickness while accounting for depth perception of the camera with an accuracy of ±0.038 mm. The computer-vision system was capable of measuring color over a particular region comparable to a colorimeter, however at the cost of accuracy.

4.1 INTRODUCTION

Computer-vision technology is capable of producing fast, objective results for the food industry (Sun 2004). The measurements from a camera are not usually comprehensive to the food industry because the measurement from the camera is the spatial distribution of intensities which forms an image. An image can be represented as a matrix of red, green and blue channels (RGB) or hue, saturation, and intensity (HSI) channels, each having 256 intensity levels for a 24 bit image. Methods have been developed to extract useful information from an image such as color and other intensity measurements and distance,

area and other spatial measurements (Russ 1992). Specifically, RGB values are not as useful to the food industry as the Commission internationale de l'éclairage (CIE) L*a*b* color measurements. Mathematical conversions from RGB to L*a*b* have been developed but require the use of standard illuminants during image capture which may not always be available. Geometric measurements from a computer-vision system are often measured as the number of pixels which represent an object. This representation could be the number of pixels in a line, or the total number of pixels representing an area. To be useful to the food industry, these pixel representations must be converted to standard unit measurements. Therefore, relationships between camera color measurements (RGB) and real color measurements (L*a*b*) need to be established. Relationships between pixel measurements and geometric measurements must also be determined.

A problem occurs for industries when more than one computer-vision system is used because of varying camera hardware, lighting, and computer hardware, which make measurements difficult to compare. Differences in optics and camera placement have effects on geometric pixel representations. Light placement and spectrums have effects on color reproducibility and spatial consistency. The camera settings vary depending on the manufacturer and can represent different levels of the same attribute since camera settings are not universal. It is important that colorimetric and spatial calibrations be conducted so that results from varying systems can be compared.

The specific objectives of this study were to address common problems in computer-vision systems and develop and test methods to calibrate a camera. These problems included lens distortions, non-uniform illumination, brightness, contrast, white

balancing, spatial and color measurements. These methods will allow differing computer-vision system cameras and configurations to be standardized so that image parameters can be compared. The parameters of interest are pixel size in relation to distance and area, hue-saturation-intensity values in relation to CIE L*a*b* color values. From these parameters, many other image features can be extracted.

4.1.1 Lens Distortion

Image distortion is any deviation in the image from the actual projection of an object. The most common distortion is radial and can be classified into two categories; barrel and pincushion distortion. To obtain a wide field of view at a lower cost, a full frame fish-eye lens is commonly used (Shah and Aggarwal 1996). Fish-eye lenses are able to map a wide object onto a small image sensor. The use of a fish-eye lens often creates barrel distortion because the image magnification decreases with distance from the optical center (Shah and Aggarwal 1996). To make accurate measurements of distance and area within a digital image, it is important that lens distortions be compensated within a photographic field. This problem can be resolved through the use of larger lenses or by a mathematical equation proposed by Brown (1966) implemented in the image analysis software. To determine the mapping of distorted points to undistorted points, Brown (1966) proposed the equation:

$$x' = x + (x - x_p)(K_1 r^2 + K_2 r^4 + K_3 r^6 + \cdots) + \left[P_1\left(r^2 + 2(x - x_p)^2\right) + 2P_2(x - x_p)(y - y_p)\right][1 + P_3 r^2 + \cdots] \quad (2)$$

$$y' = y + (y - y_p)(K_1 r^2 + K_2 r^4 + K_3 r^6 + \cdots) + \left[2P_1(x - x_p)(y - y_p) + P_2\left(r^2 + 2(y - y_p)^2\right)\right][1 + P_3 r^2 + \cdots] \quad (3)$$

where:

$$r = \sqrt{\left(x - x_p\right)^2 + \left(y - y_p\right)^2} \quad (4)$$

Where K_n are coefficients of radial distortion, P_n are coefficients of tangential distortion, (x_p,y_p) define the optical center of the lens, (x, y) define the distorted image point, (x', y') are the undistorted image points, r is the distance between a distorted point and the center of the image, and '…' indicates an infinite series. This research used a subroutine provided by the Vision Acquisition Assistant 8.5 (National Instruments, Texas, USA) to automatically determine the coefficients required and apply the appropriate corrections.

4.1.2 Non-Uniform Illumination

Non-uniform illumination can distort color measurements and inhibit the ability to accurately detect edges within a digital image. Single point or multiple point sources are often a cause of non-uniform illumination. Ideally, having a lighting setup that can provide uniform illumination would produce optimal image quality. To reduce costs however, it is often simpler to correct the images using software. Since images are two-dimensional in nature, a method of correcting non-uniform illumination is to model the intensity plane of an image with a two-dimensional polynomial function (Russ 1992) and will be used in this research.

4.1.3 Area and Thickness Measurements

Three-dimensional imaging requires more than one perspective on the object of interest. To image an apple slice, two cameras with perpendicular views can allow for direct measurements of surface area and thickness. After spatial calibration and distortion correction, the surface area represented by a single pixel could be determined. Depth perception to the camera however is often a problem. Depth perception is a non-linear

component that affects perceived areas and thicknesses. The object must either be placed at the same distance from the camera, or statistic models can be developed to account for the distance from the camera, and implemented in software.

4.1.4 Brightness, Contrast and White Balance

To maximize image quality and dynamic range, the basic camera settings should be optimized to achieve clear picture and color quality. To maximize the dynamic range of the intensity, brightness and contrast levels should be determined. Brightness is an intensity measurement which is often used to determine which intensity level is considered black. Contrast is the change in intensity per unit of brightness. Brightness and contrast can be set using a neutral reference black and white color object.

White balance is used to adjust the camera perception of white objects. Digital cameras often have manual or automatic white balance controls. Using a neutral white or grey color reference card, each color channel can be adjusted to give the same intensity. Once set, the white balance controls should be fixed to prevent any changes in the white balance, when samples are placed in the photographic region.

4.1.5 Color Measurements

Human color perception is very subjective and is based on surrounding colors. Computer-vision doesn't depend on the color of surrounding objects and can objectively measure color tristimulus values, usually red-green-blue or hue-saturation-intensity. The food industry usually makes measurements using CIE L*a*b* color representations. The conversion between hue-saturation-intensity and CIE L*a*b* can be performed using the following equations:

$$Hue = \tan^{-1}\left(\frac{b^*}{a^*}\right) \quad (5)$$

$$Saturation = \sqrt{a^{*2} + b^{*2}} \quad (6)$$

$$Intensity = kL^{*} \quad (7)$$

The output from a digital camera however is not in the range required for these equations. The correlated color temperature of the light source also has effects on color measurements. Standard illuminants can be selected to make the conversion easier, as mathematical methods such as chromatic adaptation matrices have been developed for such a conversion. This research proposes to use modelling statistics to determine the chromatic adaptation required for a non-standard light source using a known color standard, the Gretag MacBeth colorchecker. This will provide measurements from the digital camera which are comparable to a colorimeter.

4.2 METHODS

4.2.1 The Drying Apparatus

The photographic region was inside a tray dryer (model: UOP8, Armfield Ltd., Ringwood, UK). The region was illuminated by two light emitting diodes (LED) with chromaticity values of x=0.33 and y=0.33 and light intensity of approximately 400 lux in the center of the region. The top camera (model: Unibrain Fire-I, Unibrain Inc., San Roman, CA, USA) was placed 20 cm above the top tray and the side camera (model: ImagingSource DFK31AF03, The Imaging Source LLC, Charlotte, NC, USA) was pressed up against the glass window, 14 cm from the center of the dryer making the two cameras 90° to each other. Both were interfaced using an IEEE 1394 Firewire interface card. The imaging software was developed using Labview 8.5 with the Vision Development Module 8.5 (National Instruments) on an HP Compaq DC7800p (Intel Core 2 Duo E6750 @ 2.66 GHz, 2 GB RAM, HP, USA).

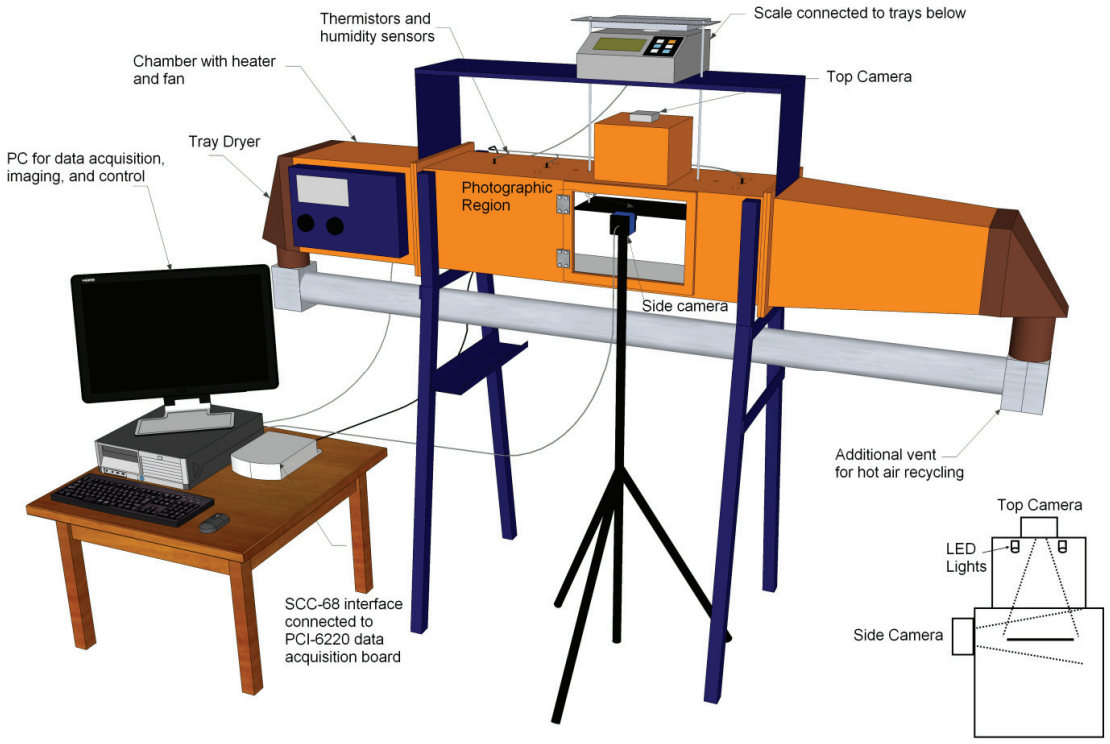

Figure 4.1 Diagram of drying apparatus, sensors, and imaging equipment with cross-section of imaging region.

4.2.2 Spatial Distortion Correction

To correct spatial distortion, a Vision Acquisition Assistant subroutine was used to capture an image of a grid of dots with a spacing of 5 mm. The subroutine calculated the necessary information and stored the image as well as the calibration information as a portable network graphic (PNG) file. This image can be recalled and the calibration information applied to subsequent images.

The spatial correction subroutine indicated that there should be approximately 3.125 mm per 10 pixels and was able to correct the non-linear distortion caused by the lens (Figure 4.2).

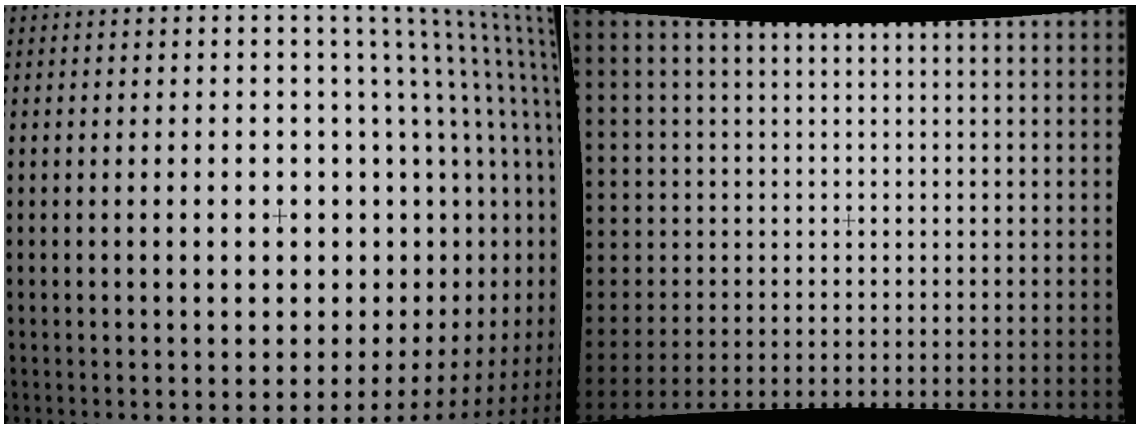

Figure 4.2 Example of spatial distortion uncorrected (left) and corrected (right) from the computer-vision system

4.2.3 Non-uniform Illumination Correction

White balance of the camera was assessed using the ColorChecker White balance card (X-rite, USA). With the card illuminated in the photographic region, the white balance settings were adjusted manually until each color channel measurement was the same. Once white balancing was completed, the ColorChecker Passport (X-rite, USA) was placed in the photographic region. A LabVIEW algorithm swept the camera brightness setting and measured the average intensity of the black color of the ColorChecker. Once the algorithm detected that the average intensity was no longer zero, the algorithm decreased the brightness by one and the brightness setting was recorded. The ColorChecker White Balance card was replaced in the photographic region to determine the gain setting. The gain was determined using a LabVIEW algorithm that swept through the camera gain settings and measured the maximum pixel intensity of the image. Once the maximum pixel intensity reached 253 (to avoid image saturation), the gain value was stored.

Non-uniform illumination was assessed using the ColorChecker White Balance card. An image was captured and the intensity plane was extracted and converted to a

matrix of numbers. The maximum intensity in the matrix was found. Scale factors were determined for each individual pixel to bring the intensity up to the maximum value. These scale factors were stored in a matrix of 640 x 480 elements. This matrix was applied to the intensity plane of subsequent images to provide uniform intensity, without altering the chromaticity of the object.

The non-uniform illumination, whether from the lens or the lighting, was corrected (Figure 4.3).

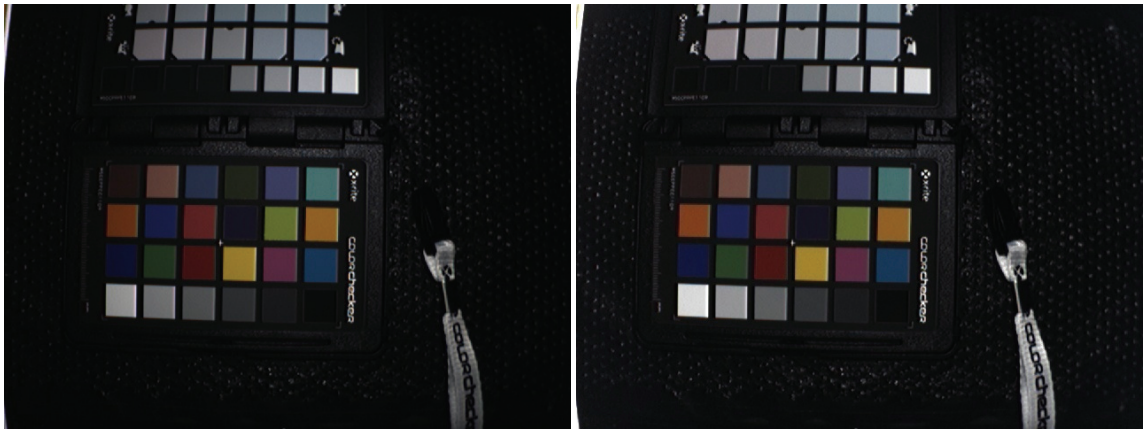

Figure 4.3 Example of Non-uniform illumination (left) and corrected uniform illumination (right) using the colorchecker passport

4.2.4 Surface Area and Thickness Calibrations

White circles of varying diameters (40-70mm in steps of 5mm) were printed using computer aided drafting software on a black background using a Samsung ML 2010 LaserJet printer (Figure 4.4). A random circle was chosen and placed in the region of interest in front of the top camera and an image was captured for analysis. This process was repeated until each circle was imaged three times. Each image was segmented and the area in pixels was determined. Regression analysis was used to determine a linear model to relate image analysis measurements to real-world measurements in squared millimeters.

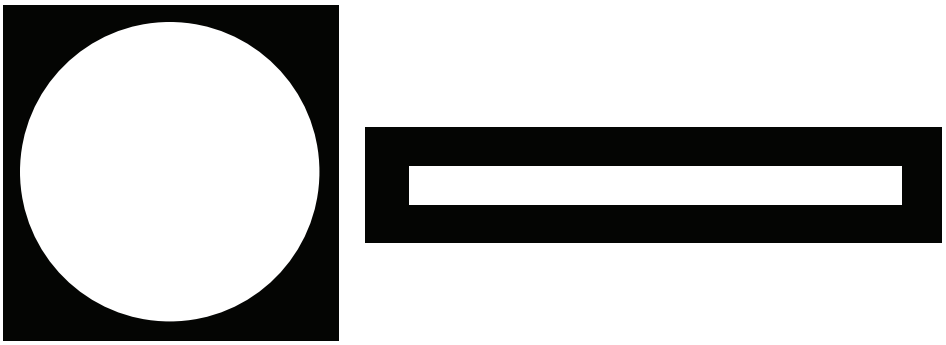

Figure 4.4 Samples of circle used for calibrating the area measurements (left), and a line used for calibrating the thickness measurements.

White lines of varying thicknesses (1mm to 5 mm in steps of 0.5 mm) were printed using computer aided drafting software on a black background using a Samsung ML 2010 LaserJet printer (Figure 4.4). A random line was chosen and placed at a specified distance (5 mm to 20 mm in steps of 3 mm) from the side camera in the region of interest and an image was captured for analysis. This process was repeated until each line was imaged three times. Each image was analyzed and the thickness in pixels was determined using edge detection. Regression analysis was used to determine a non-linear model to relate image analysis measurements to real-world measurements in millimeters.

4.2.5 Color Calibrations

A ColorChecker Passport (X-rite, Grand Rapids, MI, USA) was placed in the center of the field of view for the top camera (Figure 4.5). Three images were captured with the ColorChecker Passport in a different position for analysis. Each color was measured using the digital camera in the Hue-Saturation-Intensity (HSI) color space. Each color was then measured with a Minolta Chroma Meter (model: CR-300, Konica Minolta Sensing, Inc., Ramsey, NJ, USA). The measurements from the colorimeter were converted to the HSI color space. Stepwise linear regression was used to determine the model to convert the hue and saturation camera measurements to the colorimeter

measurements. Linear regression was used to determine a model to convert the intensity measurement to L* measurements.

Figure 4.5 X-rite ColorChecker Passport for color calibration.

4.3 RESULTS

4.3.1 Area Measurements

A high correlation was found between area calculated with caliper measurements and area measurements from the computer-vision system using circles printed on paper (R^2 = 0.999, $p < 0.0001$). Regression analysis indicated that the coefficient and the intercept were significant. The coefficients for the model are summarized in table 4.1. The model used for the conversion was a simple linear model:

$$\hat{y} = \beta_0 + \beta_1 x \tag{8}$$

where $\hat{y}$ is the measurement in pixels and x is the area in square millimeters.

Table 4.1 Regression coefficients to calculate area from the image.

Coefficient	Value	p-value
β_0	543.55	0.0035
β_1	10.01	< 0.0001

The comparison between the computer-vision measurements after converting to square millimeters and the area calculated from the caliper measurements shows that the two measurement methods were equal (Figure 4.6).

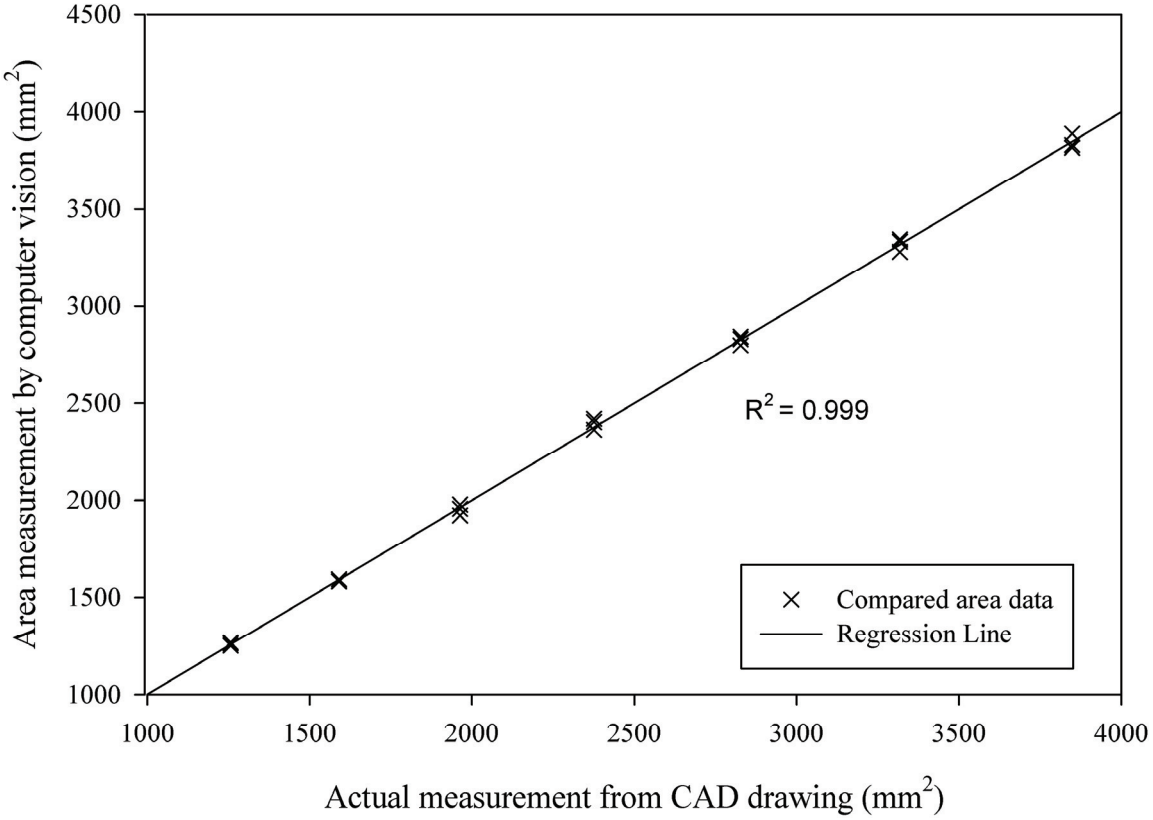

Figure 4.6 Comparison of area measurements from computer-vision and CAD measurements.

4.3.2 Thickness Measurements

To relate the perceived thickness values in pixels to real-world units of millimeters, an exponential model is proposed. The relationship between the perceived height from the

camera and distance of an object from the camera is asymptotic. An exponential model used in conjunction with a linear model could account for optical differences between an ideal camera and the camera used in this system, where a hyperbolic pinhole model may not. Data collected at a distance of 5 mm and 20 mm from the side camera was removed since it was not within the camera lens' depth of field. Non-linear regression analysis was used with the following model:

$$\hat{y} = \theta_1 + \theta_2 x_1 x_2 e^{(-\theta_3 x_1)} \tag{9}$$

where $\hat{y}$ is the predicted value of thickness in pixels, x_1 is the distance from the camera in millimeters, and x_2 is the thickness measured in millimeters. The values for the parameters of the model are shown in table 4.2.

Table 4.2 Model parameters for calculating the thickness from the image.

Parameter	**Value**	**Approximate 95% Interval**	
		Lower Limit	Upper Limit
θ_1	0.8306	0.4643	1.1969
θ_2	3.7564	3.6224	3.8904
θ_3	0.1950	0.1909	0.1991

The approximate 95% confidence interval indicates that the parameters are significantly different than zero. Using this mathematical model, the data collected from the computer-vision system was compared to the caliper data showing that the two methods were equal (Figure 4.7).

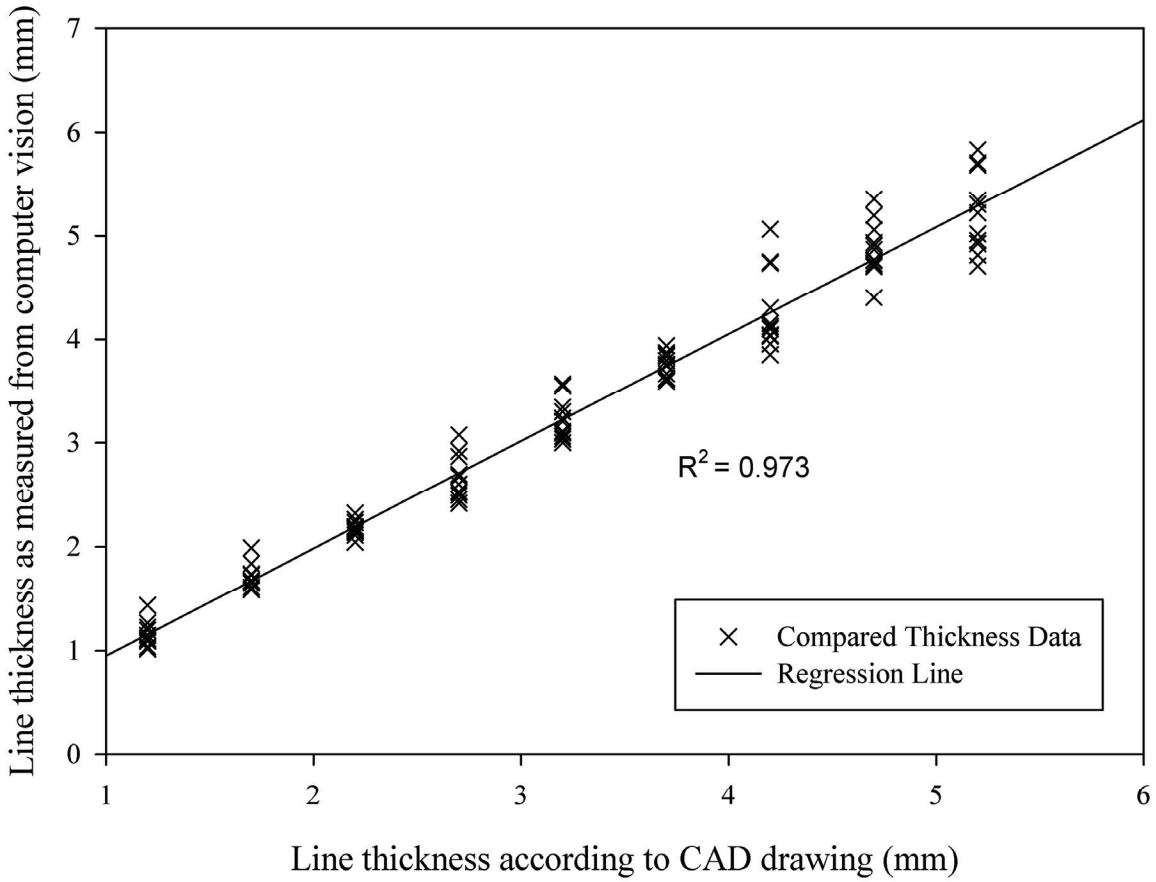

Figure 4.7 Comparison of thickness measurements calculated by image analysis and with the caliper.

4.3.3 Color Measurements

The conversion between the Hue-Saturation-Intensity measurements from the camera and the CIE L*a*b* from the Minolta colorimeter was found by determining empirical regression models between Intensity and L*, and Hue and Saturation with a* and b*.

Intensity

Linear regression revealed a R^2 value of 0.9006 between the intensity calculated from the Minolta L* measurements and the camera's intensity measurement. The fitted model was:

$$\hat{y} = \beta_0 + \beta_1 x + \beta_2 x^2 \quad (10)$$

where y is the measurement from the colorimeter and x is the measurement of intensity from the camera. The coefficients are shown in table 4.3.

Table 4.3 Results of regression analysis for intensity.

Coefficient	Value	p-value
β_0	12.86	<0.0001
β_1	0.766	<0.0001
β_2	-0.00178	<0.0001

Hue

Stepwise regression revealed that several polynomial terms were not significant. Linear regression revealed a R^2 value of 0.9956 between the hue calculated from the Minolta a* and b* measurements and the camera's hue measurement. The fitted model was:

$$\hat{y} = \beta_0 + \beta_1 x + \beta_2 x^2 + \beta_3 x^7 + \beta_4 x^8 + \beta_5 x^9 \quad (11)$$

where y is the measurement from the colorimeter and x is the measurement of intensity from the camera. The coefficients are shown in table 4.4.

Table 4.4 Results of regression analysis for hue angle.

Coefficient	Value	p-value
β_0	30.65	<0.0001
β_1	2.54	<0.0001
β_2	-0.016	<0.0001
β_3	6.68×10^{-13}	<0.0001
β_4	-5.38×10^{-15}	<0.0001
β_5	1.11×10^{-17}	<0.0001

Saturation

Stepwise regression revealed that only the intercept and linear term were significant. Linear regression revealed a R^2 value of 0.9432 between the hue calculated

from the Minolta a* and b* measurements and the camera's hue measurement. The fitted model was:

$$\hat{y} = \beta_0 + \beta_1 x \tag{12}$$

where y is the measurement from the colorimeter and x is the measurement of intensity from the camera. The coefficients are shown in table 4.5.

Table 4.5 Results of regression analysis for color saturation.

Coefficient	Value	p-value
β_0	10.65	<0.0001
β_1	0.3404	<0.0001

4.3.4 L*a*b* Comparison

After developing the models for HSI, the following measurements from the computer-vision system were converted to L*a*b* and comparisons were made. The coefficients for each linear model are shown in table 4.6.

Table 4.6 Regression coefficients to compare L*a*b* from computer-vision and the colorimeter.

Color Parameter	Coefficient	Value	p-value
L*	β_0	-0.0000259	>0.5 ($\beta_0 = 0$)
	β_1	1.000	>0.5 ($\beta_1 = 1$)
a*	β_0	-0.5989	0.330 ($\beta_0 = 0$)
	β_1	0.9672	0.162 ($\beta_1 = 1$)
b*	β_0	-2.256	0.090 ($\beta_0 = 0$)
	β_1	0.963	0.257 ($\beta_1 = 1$)

These results indicated that there was not a significant difference between the L*, a* and b* measurements from the Minolta colorimeter and the computer-vision system.

4.4 Discussion

In the area model, the intercept was significant, which indicates that there is systematic error in the measurements of 543.55 pixels. Developing a conversion between pixel measurements and caliper measurements will have to take this error into account. The slope indicates that there are 10.01 pixels in one square millimeter. The correlation between area measurements from image analysis and from the caliper was found to be R^2=0.999. The intercept in this comparison was found to be not significantly different than 0 ($p > 0.05$), and the slope not significantly different than 1 ($p > 0.05$).

$$Area_{mm^2} = 0.09985 Area_{Pixels} - 52.45 \quad (13)$$

In the thickness model, the intercept indicates that there was systematic error in this experiment which could be due to the observation that the lines used as experimental units may have been a little thicker than what was measured. Further modifications to the model are needed for the model to be used in a programming environment to convert the distance from the camera in pixels to millimeters for this model. The model can easily be solved for the height in millimeters for a given height in pixels from the side camera. The model to convert from the height in pixels and distance from the side camera in millimeters to a height in millimeters is as follows:

$$h_{mm} = \frac{h_{Pixel} - 0.8306}{3.7564 d_{mm} e^{-0.195 d_{mm}}} \quad (14)$$

The correlation between thickness measurements from image analysis and from the caliper was found to be R^2=0.973. The intercept in this comparison was found to be not significantly different than 0 ($p > 0.05$), and the slope not significantly different than 1 ($p > 0.05$).

A slope of 1 and an intercept of 0 for both measurement types indicate that the effects of the systematic error are negligible on the actual measurement with image analysis. For the current vision system, to measure the area of a flat object, equation 13 can be used to convert the pixel measurements to square millimeters with an accuracy of ±11.01 mm^2 ($\alpha = 0.05$) for flat objects and equation 4 can be used to convert the thickness pixel measurements and distance measurements to millimeters with an accuracy of ±0.038 mm ($\alpha = 0.05$).

4.4.1 Color Measurements

Since there was no significant difference between any of the color measurements from either the colorimeter or the computer-vision system, the computer-vision system could be used for its lower cost and spatial advantages. However, the trade-off is measurement error. The standard deviation for color difference measurements is approximately 4.22 for the computer-vision system, where the Minolta CR-300 colorimeter specifies a standard deviation of 0.07 for similar measurements (Konica Minolta Sensing, Inc., Ramsey, NJ, USA). The standard deviation for the computer-vision system could easily be improved by taking more color measurements with the camera to increase accuracy.

4.5 Conclusion

Currently there is no method of comparing measurements between computer-vision systems because there is no common standard. The methods outlined in this chapter will make such comparisons possible within industry, where multiple computer-vision systems are used. The computer-vision system is capable of providing accurate measurements of surface area and thickness of apple slices. The computer-vision system

does have the ability to make many color measurements in a single image at the cost of accuracy to a colorimeter.

CHAPTER 5 ANALYSIS OF APPLE SLICE VOLUME AND TEXTURE USING A COMPUTER-VISION SYSTEM

ABSTRACT

Rapid, non-contact measurements of volume and texture are very useful to the food industry. The present study was conducted to assess the ability of the computer-vision system to measure volume and food texture characteristics of apple slices during the drying process. Apple slices were dried at three different temperatures (40, 60, 80 °C) while their volume was measured with both the computer-vision system and a caliper. The food texture was assessed according to the moisture content and image texture features. The computer-vision system was able to measure the volume of the apple slices; however, the volume was not a good indicator of the end of drying because of porosity development. Image texture features were a good indicator for determining the end of drying process, but could not be related to the physical texture of the apple slices.

5.1 INTRODUCTION

Drying is a process used to remove moisture from food products as water can affect the safety and stability of stored food products. The conventional technique for determining the end of drying is to monitor the moisture content and to stop the drying process when the moisture content reaches equilibrium. Accelerated growth of bacteria occurs at high levels of water activity with essentially no physical parameters of food products remaining unaffected by the moisture content (Vos and Labuza 1974; Lewicki, 2004). Temperature dependent correlations also exist between water activity and moisture content (Thompson 1972). Prothon and Ahrné (2004) have used the Guggenheim,

Anderson and De Boer model (GAB) to correlate moisture content with water activity in apples during osmotic dehydration (Prothon and Ahrné 2004). The model is as follows:

$$X = \frac{X_0 k C a_w}{[(1-ka_w)(1-ka_w-kCa_w)]} \quad (15)$$

Where X is the moisture content (% dry basis), a_w is the water activity, X_0 equals the mono-layer water and k and C are constants.

Water activity is a better indicator of desirable texture for snack foods than moisture content (Katz and Labuza 1981). Crispness intensity as indicated by water activity for pop corn and moisture as indicated by water activity for popcorn, puffed corn curls, saltine crackers and potato chips were not extended to apple slices (Katz and Labuza 1981).

This thesis study attempted to study the possible use of a computer-vision system to evaluate visual characteristics of apple slices, such as volume and image texture, and compare these to moisture content and other food quality characteristics. This evaluation would enable the development of non-contact parameters which could indicate the end of drying.

5.1.1 Volume Measurements

Shrinkage, density, and porosity are commonly measured directly with bulk (geometric) volume which is defined as the space occupied by both particles and voids within the material (Webb 2001). Pycnometry and buoyancy are two manual methods used to quantify bulk volume based on liquid displacement (Lozano et al. 1980; American Society for Testing and Materials 2004a). Periodic sampling is labor intensive and the procedure for measuring volume is destructive to the samples. However, a non-contact and non-destructive alternative is image analysis which is also capable of

performing bulk volume measurements (Gunasekaran 2000; Mittal 1996). Imaging is a preferred method for food quality control in that contamination and destruction of food items is avoided (Lu and Sun 2000). A single camera can provide bulk volume estimation of regularly-shaped objects, such as cylinders and ginseng roots (Deltel, et al. 2001; Fernández et al. 2005; Martynenko 2006), while computed tomography, laser light projection or stereoscopic imaging is required for irregularly-shaped objects, such as fruit slices (Ruff et al. 1995; Nishino et al. 2000; Pintavirooj and Sangworasil 2002; Lee 2002; Lee et al. 2006). However, computed tomography is limited by the processing resources and cost (Russ 2005). Stereo imaging is a more cost effective method used for bulk volume measurements of three-dimensional objects. Therefore, stereo imaging was the method used to measure the bulk volume of apple slices in this research.

5.1.2 Texture Measurements

Texture, defined as a sensory property detected by humans using senses of touch and pressure, is a multi-parameter attribute related to the structure of the sample (Szczesniak 2002). Crispness is a desirable characteristic of snack foods for consumers (Fillion and Kilcast 2002; Roudaut et al. 2002; Joshi et al. 2007). The relationship between food texture perception and food structure is important to understand, especially for the purpose of developing texturally attractive foods (Wilkinson et al. 2000). For fried tortilla chips, the perception of crispness, a parameter of texture, is directly related to porosity, a parameter of structure (Kawas and Moreira 2001).

Crispness and texture have been quantified by both instrumental and sensory approaches (Roudaut et al. 2002). Puncture tests on potato chips using a texture analyzer demonstrated that crispness was a function of water activity, while mechanical analyses

of crackers indicated that the initial slope of a force-deformation curve was a good indicator of crispness (Garayo and Moreira 2002; Katz and Labuza 1981). Peak force, mechanical work, and cohesiveness were also significant indicators of crispness for popcorn (Katz and Labuza 1981). Therefore, based on the results of previous research, peak force, area under the curve (mechanical work), and initial slope measurements of the force-deformation curve were used as crispness indicators for dried apple slices in this research.

Image texture is the perceived changes in scattered light from structural changes in the surface of an object (Russ 2005). A common method used to evaluate image texture is by use of the gray-level co-occurrence matrix (GLCM). The GLCM provides co-occurrence probabilities and other statistics which can be useful for calculating texture features. These pair-wise probabilities are dependent on inter-pixel spacing and direction. The co-occurrence probability can be calculated by the following equation:

$$C_{ij} = \frac{P_{ij}}{\sum_{i,j=1}^{G} P_{ij}} \tag{16}$$

Where C_{ij} is the co-occurrence probability of the pattern represented by P_{ij}, and P_{ij} is the number of occurrences a particular pattern is observed between two gray levels in the given direction and distance, and G is the number of gray levels the image will support. Statistics are then applied to the matrix to generate the texture features (Clausi 2002).

When dealing with color images, a color plane must be extracted to convert the image from a color image to a grayscale image. This study will use the hue-saturation-intensity (HSI) color planes. The textural features will therefore be identified by a color plane and a reference number. For example, feature 1 will be noted as H1 when

calculated from hue, S1 from saturation, and I1 from intensity. The textural features that will be investigated are outlined in Table 5.1.

Table 5.1 The statistic equations of textural features (Harlick 1979).

Textural feature	Description	Equation
F1	Angular second moment (Uniformity)	$\sum_{i=0}^{N-1}\sum_{j=0}^{N-1} p(i,j)^2$
F2	Contrast	$\sum_{\lvert i-j\rvert=0}^{N-1}(i-j)^2\sum_{i=0}^{N-1}\sum_{j=0}^{N-1} p(i,j)$
F3	Sum of squares	$\sum_{i=0}^{N-1}(i-\mu)^2\, p_x(i)$
F4	Correlation	$\frac{\sum_{i=0}^{N-1}\sum_{j=0}^{N-1} i\cdot j\cdot p(i,j)-\mu^2}{F3}$
F5	Product moment	$\sum_{i=0}^{N-1}\sum_{j=0}^{N-1}(i-\mu)(j-\mu)p(i,j)$
F6	Inverse difference moment	$\sum_{i=0}^{N-1}\sum_{j=0}^{N-1}\frac{p(i,j)}{1+(i-j)^2}$
F7	Entropy	$\sum_{i=0}^{N-1}\sum_{j=0}^{N-1} p(i,j)\ln p(i,j)$
F8	Sum entropy	$\sum_{k=0}^{2N-2} p_{x+y}(k)\ln p_{x+y}(k)$
F9	Difference entropy	$\sum_{k=0}^{N-1} p_{x-y}(k)\ln p_{x-y}(k)$
F10	Information correlation1	$\frac{F_7 - HXY1}{HX}$
F11	Information correlation2	$\left[1-e^{-2(HXY2-F7)}\right]^{1/2}$
		$HX = \sum_{i=0}^{N-1}\sum_{j=0}^{N-1} p_x(i)\ln p_x(i)$
		$HXY1 = -\sum_{i=0}^{N-1}\sum_{j=0}^{N-1} p(i,j)\ln\left[p_x(i)p_x(j)\right]$
		$HXY2 = -\sum_{i=0}^{N-1}\sum_{j=0}^{N-1} p_x(i)p_x(j)\ln\left[p_x(i)p_x(j)\right]$

μ is the mean intensity level in a particular sub-region; and p(i,j) is the $(i,j)^{th}$ entry in a normalized GLCM. $p_x(i)$ and $p_y(j)$ were obtained by summation of GLCM values along the i^{th} row and the j^{th} column of p(i,j), respectively.

$p_{x+y}(k)$ and $p_{x-y}(k)$ were calculated using are given as:

$$p_{x+y}(k)=\sum_{i=0}^{N-1}\sum_{j=0}^{N-1} p(i,j); i+j=k, k=0,1,\cdots,2N-2 \qquad p_{x-y}(k)=\sum_{i=0}^{N-1}\sum_{j=0}^{N-1} p(i,j); i-j=k, k=0,1,\cdots,N-1$$

5.2 MATERIALS AND METHODS

The experiment was conducted in three parts: (i) the desorption isotherm of the apple tissue was determined, (ii) the drying time according to volume from the computer vision system was assessed, and (iii) the drying time according to image texture measurements, as well as correlations between image texture and physical texture were assessed.

5.2.1 Common Preliminary Procedures For All Experiments

The drying experiments were performed in a tray dryer, modified for drying in the range of temperatures 40 °C to 80 °C. For each experiment, the tray dryer was primed at the specified temperature (40, 60 or 80 °C). The air velocity was set at 0.9 m/s. The tray dryer was considered primed when the controller virtual instrument (VI) indicates a stable reading (±0.5 °C). The air velocity was measured with a vane type thermo-anemometer (WDCFM8912, General Tools & Instruments, New York, USA) with resolution of 0.1 m/s and 5% accuracy prior to the experiments. The lights inside were turned on 10 minutes prior to the experiment to ensure a consistent light spectrum. A LabVIEW subroutine (dryer main program.vi) monitored and recorded the temperature, humidity, and weight throughout each experiment. The program also recorded images for further analysis.

5.2.2 Methods to Determine Moisture-Desorption Isotherms

The tray dryer was primed at 40 °C, 60 °C, or 80 °C. Fresh apples (cv 'Empire') were sliced to 2.0 mm thickness using the Waring FS150 Food Slicer (Waring, USA). Apple slices were chosen from the center of the apple and weighed on a separate scale (Symmetry ECII-4000, Cole-Parmer, USA) having a resolution of ±0.1 g. After the initial measurements, all apple slices will be immediately moved to the tray dryer. Three slices

were placed on a tray that was attached to a scale. Fifteen slices were placed on Teflon sheets on the stationary tray in the dryer for sampling.

A LabVIEW VI recorded the temperature and humidity and displayed the approximate volumetric water content every 2 minutes. Samples were taken at various values of moisture content for water activity measurements throughout the drying process. The apple sample was made into powder with a coffee grinder and placed in the water activity meter (Novasina, Model: ms1 Set aw, Geneq Inc. Quebec, CA). Once no mass changes over the duration of one hour were observed, the process was considered completed and the final sample was taken for measurements. The slices on the top tray were removed from the dryer for final weighing. The samples were dried for 24 hours at 105 °C to determine the dry mass for moisture content calculations.

The relationship between water activity and moisture content and temperature was determined using non-linear regression (SAS, SAS Institute, Cary, NC, USA). The coefficients of the model were compared to determine if statistically significant differences existed between the different temperatures.

5.2.3 Methods to Assess Apple Slice Volume

The tray dryer was primed at 40 °C, 60 °C, or 80 °C. Fresh apples (cv 'Golden Delicious') were sliced to a thickness of 5 mm using the Waring FS150 Food Slicer (Waring, USA). Apple slices were chosen from the center of the apple and weighed on a separate scale (Symmetry ECII-4000, Cole-Parmer, USA) having a resolution of ±0.1 g. After the initial measurements, three apple slices were immediately moved to the tray dryer. These apple slices were placed on a sheet of black Teflon with designated marks

on the top tray to be weighed and imaged. The side camera was placed using an onscreen guide to ensure optimum viewing of the apple slices.

A LabVIEW VI recorded the temperature, humidity, weight and images every 5 minutes. The images were saved in bitmap format (BMP). During the drying process, the apple slices were removed from the dryer for caliper measurements every 30 minutes. The diameter and thickness of the apple slices were measured with a digital caliper (Mastercraft) in three places and an average was calculated. Once LabVIEW recorded no mass and area changes over the duration of one hour, the process was considered complete. The slices were removed from the dryer for final weighing, diameter, and thickness measurements. The samples were dried for 24 hours at 105 °C to determine the dry mass, which was used for calculations of moisture content on the dry basis.

Once all data and images were collected, a LabVIEW subroutine (image processor main program.vi) was executed to sequentially process the images. Image processing included extracting the intensity plane from the image, applying a threshold to identify the apple slices from the image background and filtering the image to remove small objects compared to the apple slices. The image analysis program also calculated the surface area and the thickness of each apple slice in pixels. Conversion from the pixel measurements to the physical measurements was done using scaling coefficients determined from a previous experiment. Volume (V) was calculated using the surface area (A) and thickness (h) measurements and the equation:

$$V = A \cdot h \tag{17}$$

Linear regression was used to compare the caliper measurements to the volume measurements. Repeated measures analysis was used to determine when no significant

changes occurred in the volume measurements from the computer-vision system so that the drying time could be determined according to volume.

5.2.4 Methods to Assess Apple Slice Texture

The tray dryer was primed at 60 °C. Fresh apples (cv 'Empire') were sliced to a thickness of 2 mm using the Waring FS150 Food Slicer (Waring Pro, Torrington, CT, USA). Apple slices were chosen from the center of the apple and weighed on a separate scale (Symmetry ECII-4000, Cole-Parmer, USA) having a resolution of ±0.1 g. After the initial measurements, nine apple slices were immediately moved to the tray dryer. These apple slices were placed on a sheet of black Teflon with designated marks on the top tray to be weighed and imaged. The side camera was not used in this experiment.

A LabVIEW VI recorded the temperature, humidity, weight, and images every 2 minutes. Moisture contents were pre-determined for sampling (1.00, 0.90, 0.70, 0.60, 0.40, 0.26, 0.25, 0.22, 0.20, 0.17 g/g dry matter). Three of the nine apple slices were removed from varying positions in the dryer when the LabVIEW VI indicated that the approximate moisture content was reached. Samples were taken at two specific moisture contents per run. The slices were weighed and brought to a texture analyzer (TA.XT Plus, Texture Technologies Corp., New York, USA). Using a puncture test, the apple slice was broken and the peak force, area under the curve, and initial slope of the stress-strain curve was recorded. The remaining three apple slices were used to determine the actual moisture content. This process was repeated until 10 values of moisture and texture were recorded and therefore, each day was treated as a blocking factor.

Once all data and images were collected, a LabVIEW subroutine (texture analysis main program.vi) was executed to sequentially process the images. Image processing

included extracting a color plane and using the co-occurrence matrix to obtain measures of image texture. To analyze texture, each bitmap image was segmented into the six individual apple slices. The specified color plane was extracted and converted to a 64 gray level image to increase computational efficiency. The co-occurrence matrix and textural features were calculated.

Correlation analysis was used to determine if any relationships between the measurements of image texture and physical texture existed. Repeated measures analysis was used to determine when there was no significant change in image texture so that the drying time could be determined according to image texture.

5.3 Results

No significant differences in desorption isotherm coefficients with respect to temperature were observed. The coefficients for the desorption isotherm model (equation 15) are shown in table 5.2.

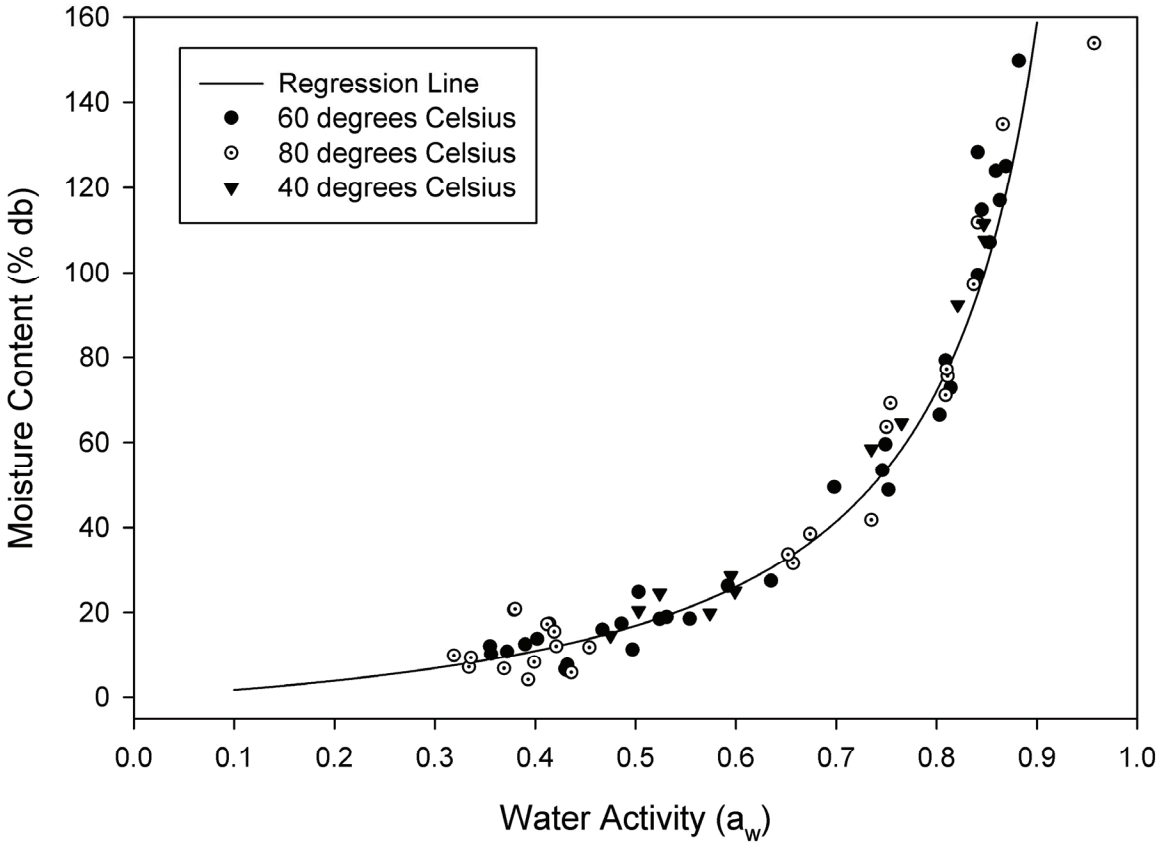

Figure 5.1 Fitted line plot of desorption isotherm with collected data of apple slices.

Table 5.2 Desorption isotherm coefficients for the GAB model.

Coefficient	**Estimate**	**p-value**
X_0	0.2492	0.002
k	0.2575	0.640
C	2.8396	<0.001

5.3.1 Volume Experiment

Regression analysis indicated that the computer-vision system can be used in place of the caliper methods to determine the volume of the apple slices ($p < 0.05$). The drying times according to the moisture and volume changes are shown in Table 5.3.

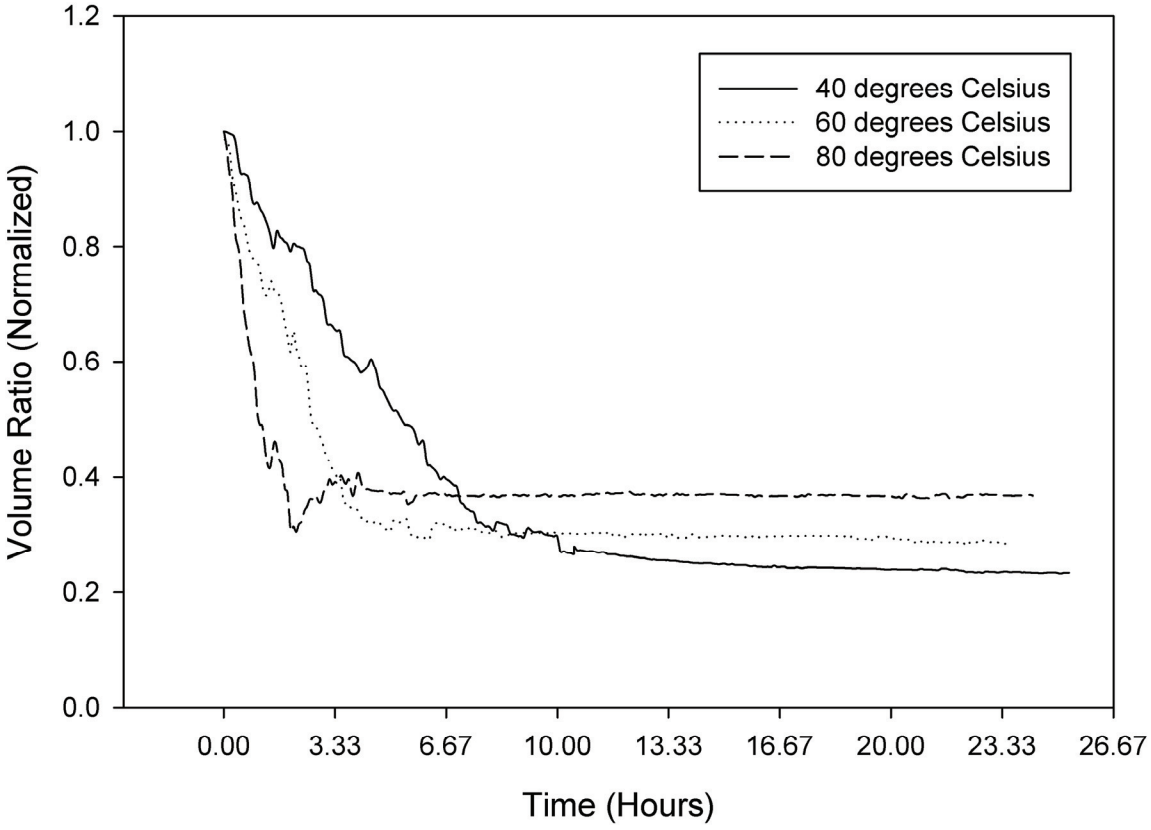

Figure 5.2 Volume ratio trends of apple slice observed during the drying process at different temperatures

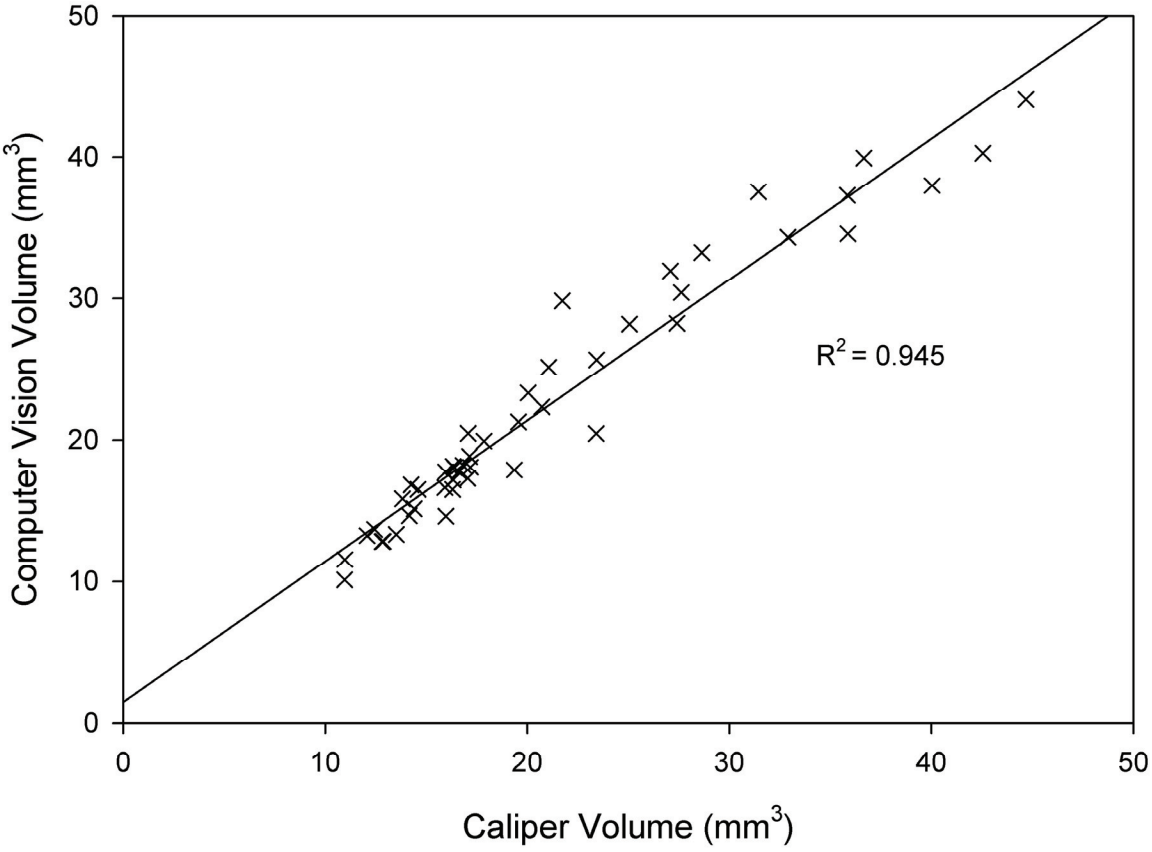

Figure 5.3 Volume measurement comparisons between the caliper and the computer-vision system.

Table 5.3 Drying times according to volume, compared to the moisture content.

Temperature	Time (Hours) from moisture	Time (Hours) From volume
40	20.67	18.08
60	16.33	8.33
80	10.33	6.41

5.3.2 Image Texture Experiment

The drying times according to the moisture content for the texture experiment was 4.31±0.313 hours and while according to the I1 texture feature, the duration was 4.42±0.125 hours. Correlation analysis indicated that a significant correlation existed between the peak force and H3 ($r = 0.500$, $p = 0.0049$), H5 ($r = 0.474$, $p = 0.0081$), S2 (r

= 0.3828, p = 0.0081) and significant correlation existed between the initial slope and H3 (r = 0.476, p = 0.0078), H5 (r = 0.559, p = 0.0013), and S11 (r = -374, p = 0.0415). The remaining image texture measurements do not correlate well with the physical texture parameters from the texture analyzer (Table 5.4). The following features did correlate well with the moisture content ($R^2 > 0.9$): H1, S1, I1, S2, I2, H3, I3, S4, I5, S9, I9. These features also had a high correlation between each feature.

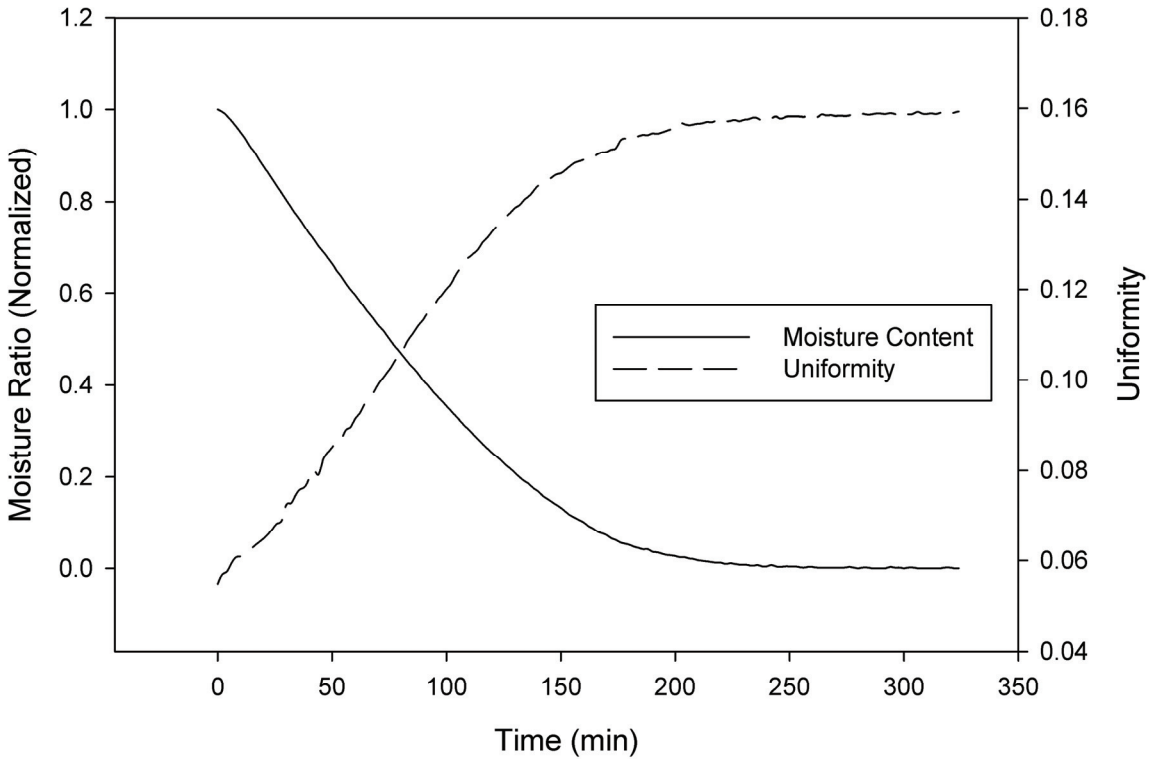

Figure 5.4 Sample plot of moisture content with uniformity from the intensity plane (Textural feature I1) with time.

Table 5.4 Correlation coefficients between physical texture features and image texture features.

Texture feature		Peak force	Area under curve	Initial slope	Texture feature	Peak force	Area under curve	Initial slope
H1	r	0.14009	0.21285	0.08214	S7	-0.10648	-0.10489	-0.0098
	p	0.4603	0.2588	0.6661		0.5755	0.5812	0.959
H2	r	-0.11732	-0.19141	0.0018	S8	-0.15029	-0.16377	-0.09813
	p	0.5369	0.3109	0.9925		0.4279	0.3872	0.6059
H3	r	0.50004	0.34524	0.47635	S9	-0.02871	0.00321	0.12265
	p	0.0049	0.0617	0.0078		0.8803	0.9866	0.5185
H4	r	-0.35024	-0.22965	-0.18949	S10	-0.03878	-0.05288	-0.20895
	p	0.0578	0.2222	0.3159		0.8388	0.7814	0.2678
H5	r	0.47414	0.33366	0.55875	S11	-0.20551	-0.21714	-0.37445
	p	0.0081	0.0716	0.0013		0.2759	0.2491	0.0415
H6	r	-0.08669	0.07728	-0.20704	I1	0.22468	0.23273	0.18926
	p	0.6488	0.6848	0.2723		0.2326	0.2159	0.3165
H7	r	0.07764	-0.08571	0.17355	I2	-0.1874	-0.14449	-0.16593
	p	0.6834	0.6525	0.359		0.3214	0.4462	0.3808
H8	r	0.04981	-0.08967	0.13018	I3	-0.03934	0.09148	-0.06814
	p	0.7938	0.6375	0.4929		0.8365	0.6307	0.7205
H9	r	0.21318	0.02327	0.28786	I4	-0.18871	-0.19093	-0.29093
	p	0.258	0.9028	0.1229		0.3179	0.3122	0.1188
H10	r	-0.00063	0.14315	-0.14096	I5	-0.04003	0.09075	-0.07144
	p	0.9974	0.4505	0.4575		0.8336	0.6334	0.7076
H11	r	0.23457	0.20107	0.0821	I6	0.04333	0.03911	-0.10858
	p	0.2121	0.2867	0.6662		0.8202	0.8374	0.5679
S1	r	0.23021	0.23409	0.19979	I7	-0.15953	-0.16098	-0.04999
	p	0.221	0.2131	0.2898		0.3998	0.3954	0.7931
S2	r	-0.3828	-0.25568	-0.29762	I8	-0.21969	-0.21999	-0.14449
	p	0.0368	0.1727	0.1102		0.2434	0.2428	0.4462
S3	r	-0.18894	0.01161	-0.13819	I9	-0.01332	-0.00517	0.13984
	p	0.3173	0.9515	0.4665		0.9443	0.9784	0.4611
S4	r	0.14634	0.13132	0.16127	I10	-0.05951	-0.04843	-0.20904
	p	0.4403	0.4891	0.3946		0.7548	0.7994	0.2676
S5	r	-0.14302	0.03538	-0.0965	I11	-0.30475	-0.29214	-0.37844
	p	0.4509	0.8528	0.612		0.1015	0.1172	0.0392
S6	r	0.0644	0.02947	-0.08155				
	p	0.7353	0.8772	0.6683				

r = pearson correlation coefficient

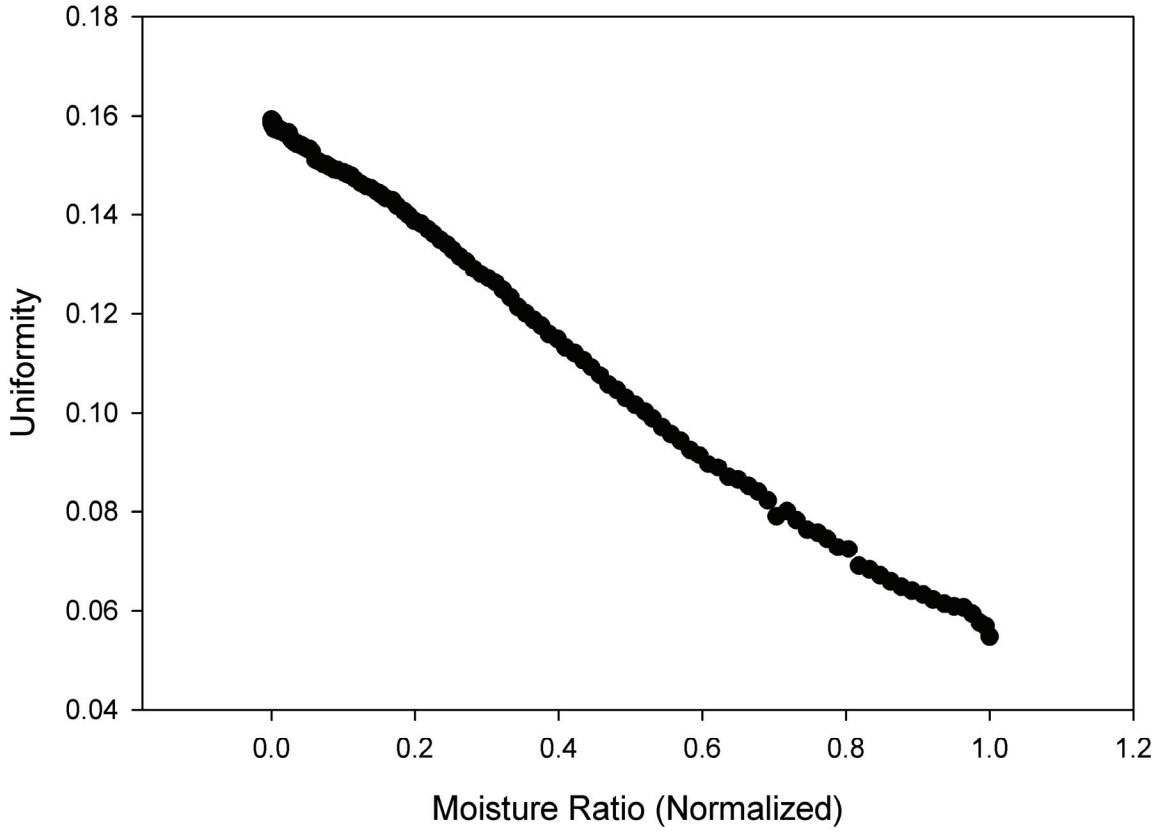

Figure 5.5 Uniformity (I1) compared to the moisture ratio

5.4 Discussion

The lack of difference between the desorption isotherm coefficients was possibly due to the method of measurement. Typically, by the time the apple slice was made into powder, the temperature of the apple tissue was approximately room temperature instead of the drying temperature. From a food product perspective, this desorption isotherm can provide information about the expected water activity when the sample is brought to room temperature after drying to a specific moisture content.

5.4.1 Volume Experiment

While the computer-vision system can be used to accurately measure the volume of the apple slices during the drying process, volume is not necessarily a good indicator of the

end of drying point because of the development of porosity. Case hardening is correlated with pore development and so shrinkage stops while moisture continues to escape.

5.4.2 Image Texture Experiment

While image texture analysis could not be used to assess the physical texture parameters of the apple slices, image texture feature I1 (Uniformity or Angular Second Moment) was a good indicator of the end of drying as it stopped changing when moisture reached equilibrium. As the surface area decreased from shrinkage and bending, more image space was given to the background, thereby creating a more uniform image and a high correlation with moisture content. This is not the case when only the apple tissue within the image was analyzed. The uniformity within the apple tissue did decrease, but did not correlate well with the moisture content.

5.5 Conclusion

It can be concluded that while the volume can be measured accurately with a computer-vision system, it should not be used as an end of drying characteristic without taking into account porosity development. Image textural features I1 can be used as an end of drying characteristic because of the close correlations with the moisture content.

CHAPTER 6 EVALUATION OF PHENOLIC COMPOUNDS AND COLOR MEASUREMENTS USING REAL-TIME IMAGE ANALYSIS DURING THE DRYING PROCESS OF APPLE SLICES

ABSTRACT

The use of computer-vision technology has rapidly increased in the fields of quality inspection, classification, and evaluation of food product quality. The objectives of this study were to examine the effects of three drying temperatures (40, 60, 80 °C) and blanching on phenolic compounds degradation and hydroxymethylfurfural (HMF) development during the thermal processing of Quinté apple slices. Color changes in the flesh and core, as well as biochemical indicators were measured over time to examine the phenolic concentrations and HMF development during the drying process. The results indicated that phenolic concentrations in the unblanched apple slices decreased for all temperatures, while no significant decreases were observed for the blanched slices. HMF also developed at 80°C, but not at 40 °C or 60 °C and blanching also promoted HMF development. Computer-vision measured additional color changes in the core which were highly correlated with HMF development ($r = -0.7908$, $p = 0.002$).

6.1 INTRODUCTION

The use of computer-vision technology has been successfully implemented in the food industry as a method of grading food products, particularly in the fields of baked goods, meat products, and fruits and vegetables (Brosnan and Sun 2004). To identify an appropriate computer-vision based parameter that can be used for determining the quality of dehydrated apple chips, relationships between computer imaging under thermal processing conditions and corresponding biochemical changes in apple tissue need to be investigated.

Hydroxymethylfurfural (HMF) is a product of the Maillard reaction which involves the reaction between an amino acid and a reducing sugar (Rosatella et al. 2011). In previous studies, thermally processed apricots and plums showed higher levels of hydroxymethylfurfural (HMF) and increased losses of phenolic compounds when processed at higher temperatures (Piga et al. 2003; Madrau et al. 2009). Phenolic compounds have also been correlated with the antioxidant capacity in fruit (Sellappan et al. 2002; Prior et al. 1998; Gil et al. 2000; Wojdylo et al. 2008; Tsao et al. 2005). HMF development in relation to color measurements was also characterized in 'Granny Smith' apple powder after thermal processing (Resnik and Chirife 1979). However, the relationship between HMF accumulation and dehydration of apple slices has not been reported.

Product appearance is a very important attribute of dried snack foods with regards to consumer perception. When apples are sliced, a brown color was observed because of enzymatic browning caused by the damaged fruit tissue. Enzymatic browning is known to cause changes in flavor and loss of nutrients (Luo and Barbosa 1997) as well as degrade the visual quality and the sensory properties in apple slices (McEvily et al. 1992). To control enzymatic browning, blanching treatments such as dipping in ascorbic acid, citric acid, sodium chloride, or calcium chloride are often used to inactivate the polyphenol oxidase (PPO) enzymes (Pizzocardo et al. 1993). Enzymatic browning in relation to PPO activity was characterized in many apple cultivars in previous work (Joshi et al. 2007). HMF development in relation to color measurements was also characterized in 'Granny Smith' apple powder after thermal processing (Resnik and Chirife 1979). However, no recent work with apple slices could be found. Therefore,

this research is focused on investigating the effect of dehydration on phenolic compound degradation and HMF development in blanched and non-blanched apple slices.

Color of a food product is quantified using a colorimeter or spectrophotometer. However, these instruments lack the ability to measure spatial characteristics of color accurately on small objects. A computer-vision system can adequately measure spatial color characteristics if the region and cameras are adequately calibrated.

The goals of this study were to: (i.) examine the effects of air temperature and blanching on phenolic degradation and HMF development during the thermal processing of apple slices and (ii) analyze any relationship between real time changes of image attributes recorded by camera and the biochemical changes of the apple slices. Color changes in the flesh and core, as well as biochemical indicators were measured over time to examine the development of HMF and phenolic degradation during processing. The information collected was used to relate image attributes to the specified biochemical indicators.

6.2 METHODS

6.2.1 Reagents and Materials

High-purity (>99%) HMF was purchased from Sigma–Aldrich (Oakville, Ontario, Canada). A stock standard solution of HMF (10 μg/mL) was dissolved in water. Intermediate solutions of 5, 1, and 0.1 μg/mL were prepared from the primary standard solution by appropriate dilution in water. Nylon syringe filters (0.45 μm) were purchased from Chromatographic Specialties Inc. (Brockville, Ontario, Canada). The apples (cv. Quinté) used in the preliminary study were purchased from a local market and were produced by Blomidon Produce Ltd. (Wolfville, Nova Scotia, Canada). The apples (cv.

Gravenstein) used in the times series study were purchased from Stirling Fruit Market (Truro, Nova Scotia, Canada) and were grown in Annapolis Valley, Nova Scotia.

6.2.2 Apple Drying Preliminary Work

Apples (Quinte) were selected from available fresh harvests. Apples were peeled and sliced into 2.0 mm thick slices using a food slicer (Model FS 150C, WaringPRO^{TM}, Torrington, CT, USA). Six blanched slices, dipped in calcium chloride (1.6%) solution at room temperature for 9 minutes, and six unblanched slices were placed in random positions on the tray. The tray was placed in the dryer at the specified temperature (40, 60, 80 °C) and duration (31 h, 20 h, 8 h respectively). The drying durations were determined by estimating the time it took for the moisture content to reach 10% dry weight at each temperature. This procedure was repeated three times for all temperatures. Once the drying process was completed, the slices were removed from the dryer. Two color measurements were taken for each slice with a Minolta CR-300 colorimeter (Konica Minolta Sensing, Inc., Ramsey, NJ, USA). The slices were made into powder using a coffee grinder (Sunbeam 6378-33, Penrose, Australia). The water activity of the powder was measured using the water activity meter (Novasina, Model: ms1 Set aw, Geneq Inc. Quebec, CA). The moisture content was also determined using gravimetric analysis by drying the apple powder at 70 °C for 72 hours. Phenolic compounds and HMF were determined by HPLC-MS-MS analysis. Antioxidant capacity was measured using Ferric-Reducing Ability of Plasma (FRAP) assay.

6.2.3 Time Series

Apples were peeled and sliced and no blanching treatment was applied. Thirty-six slices were placed on a tray for periodic sampling, while three slices were placed on a tray

attached to a scale and monitored with a computer-vision system for moisture and color analysis. The computer vision system was assigned two square regions of 225 square pixels close to the core and in the flesh for color measurements of the center apple slice. The samples were dried at 80 °C for 7.5 hours. Samples of four slices were collected every 30 minutes for 2.5 hours, after which the sampling time was increased to 1 hour for the remaining samples. Once removed from the dryer, samples were flash frozen in liquid nitrogen and stored in a freezer at -20 °C until needed for analysis. After the drying treatments were completed, all the samples were freeze dried (SuperModulo freeze dryer, Thermo Electron Corporation, NY, USA) and phenolics were extracted and analyzed using HPLC-MS-MS.

6.2.4 Instrumentation and LC/MS–MS Working Conditions

The concentrations of selected major phenolics were determined using the method described by Joshi et al. (2007). Analysis of HMF was performed with a Waters UPLC Aquity H-Class separations module coupled with a Micromass Quattro micro API MS/MS system which is controlled by MassLynx V4.1 data analysis system (Micromass, Cary, NC, USA). The column used was a Waters Acquity UPLC BEH C18 1.7 µm 2.1 x 100 mm column. A gradient elution was carried out with methanol (solvent A) and water (solvent B) at a flow rate of 0.150 mL/min. A linear gradient profile was used with the following proportions of solvent A applied at time t (min); (t, A): (0, 10%), (6, 50%), (8, 65%), (10, 90%), (15, 10%). Positive electrospray ionization (ESI+) with a triple quadrupole mass analyzer was used for analysis. The following working conditions were used: capillary voltage, 3.84 kV; cone voltage, 20.00 V. Data acquisition was performed

using Multiple Reaction Monitoring (MRM) with parent ion scanning at m/z 127 and product ion scanning at m/z 109. Samples were compared to standards.

6.2.5 HMF Extraction Procedure

Food samples were ground and homogenized using a coffee grinder (Sunbeam 6378-33, Sunbeam Corporation, Botany NSW, Australia). Half a gram of apple slice powder was weighed into 15 mL centrifuge tubes to which 6 mL of acidic water, previously adjusted to pH 1 with HCl, was added. Each tube was stirred for 1 min in a vortex mixer (Fisher Scientific, Pittsburg, PA, USA) followed by sonication (Model: 750D, ETL testing Laboratories Inc., Cortland, NY, USA) at approximately 20 kHz for 5 minutes. One milliliter of each Carrez Solution (I and II) was then added and centrifugation was performed at 4000 rpm for 10 min. The supernatant aqueous sample solution was filtered through a nylon 0.45 μm syringe filter (BD, Ontario, Canada). HMF was quantified by a calibration curve generated by the standard solutions with concentrations of 0.1, 1, 5, and 10 ppm.

6.2.6 FRAP Assay

The FRAP assay was performed according to Rupasinghe et al. (2008) with some modifications. Both the reaction reagent (FRAP solution) and the TPTZ solution were made immediately before the assay. The FRAP solution was made by mixing 300 mmol/L acetate buffer (pH 3.6), 10 mmol/L TPTZ solution, and 20 mmol/L ferric chloride solution in the ratio of 10:1:1. The Trolox standard solution was prepared by dissolving 0.025 g of Trolox in 100 mL extraction solvent (methanol) to make 1 mmol/L Trolox, and this stock solution was stored in small aliquots in a freezer (–70 °C) until needed. To obtain the calibration curve, the Trolox stock solution was diluted with

methanol to make 20, 150, 400, 600, 900, 995 μM Trolox concentrations. The FRAP analysis was performed by reacting 20 μL of blank, standard or sample with 180 μL of FRAP solution in COSTAR 96-well clear polystyrene plates (Thermo Fisher Scientific Inc., Waltham, MA). The FLUOstar OPTIMA plate reader with an incubator and injection pump (BMG Labtech, Durham, NC) was programmed using the BMG Labtech software to take an absorbance reading at 595 nm, 6 min after the injection of the FRAP solution and a shaking time of 3 s. Both the FRAP solution and the samples in the microplate were warmed to 37ºC prior to the assay. FRAP values were expressed as mmol Trolox equivalents (TE) per 100 g of sample dry matter.

6.2.7 Statistical Methods

The preliminary experimental design was a 3x2 factorial experiment with a control. The first independent variable was three levels of temperature (40, 60, and 80 °C) compared to a control (freeze drying). The second independent variable was the $CaCl_2$ blanching treatment (blanched and unblanched). Comparisons among the phenolic compounds and HMF development were done at the 5% significance level using a two way analysis of variance with Tukey's post hoc test or with the Kruskal-Wallis test with Mann-Whitney pairwise comparisons where statistical assumptions could not be verified.

The real-time experiment was a repeated measures design. The independent variable was time measured in hours after the start of the drying process (0, 0.5, 1, 1.5, 2, 2.5, 3.5, 4.5, 5.5, and 6.5 h). Repeated measures analysis was conducted to compare the phenolic profiles and HMF development over a time series of data points, using replicates as a blocking factor. Base 10 logarithmic transformations were used to satisfy the statistical assumptions of normality and constant variance for all response variables.

Least-squares means comparison was used to compare the time series points with a 5% level of significance.

6.3 RESULTS

6.3.1 Preliminary Study Results

Preliminary tests to determine the effect of blanching on phenolic degradation was significant for total phenolics only at the 80 °C drying temperature, while significant degradation occurred at all temperatures in the unblanched treatment. Chlorogenic acid, catechin, and epicatechin were preferred substrates for PPO activity in the Quinté apple slices, while other compounds did not significantly degrade (Table 6.1). Catechin and epicatechin first showed significant degradation at 60 °C when apple slices were unblanched, while significant degradation in the blanched treatment did not occur until 80 °C. Other phenolics, such as quercetin-3-*O*-rhamnoside and phloridzin did not show significant degradation in any temperature or blanching treatment. Ferulic acid, quercetin galactoside, and quercetin glucoside were detected at low levels in significant amounts not exceeding 1 mg/100g DM. A significant increase in HMF concentration was observed in both blanched and unblanched treatments at 80 °C, but was the highest with blanching (Figure 6.2).

The antioxidant capacity increased with temperature becoming significant in the blanched slices at 80 °C as measured by ORAC (Figure 6.3). FRAP indicated a decrease in antioxidant capacity at 60 °C in both blanched and unbalanced slices, although the decrease was not significant. HMF did not develop significantly until 60 °C in the blanched slices and 80 °C in the unblanched slices. There was a significant higher amount of HMF at 80 °C in the blanched slices than the unblanched slices.

Table 6.1 Phenolic concentration of apple slices after dehydration at different temperatures.

Phenolic Compounds (mg/100 g DM)*	Freeze Dried		40 °C		60 °C		80 °C	
	Blanched	Unblanched	Blanched	Unblanched	Blanched	Unblanched	Blanched	Unblanched
Phloridzin	13.5±3.9a	19.4±3.0a	13.3±1.3a	13.0±1.6a	12.3±3.0a	10.6±0.8a	16.4±0.8a	15.5±0.8a
Chlorogenic acid	67.0±4.6a	54.1±2.3ab	47.7±3.2ab	39.8±2.8b	53.6±8.2ab	37.6±4.7b	44.9±1.1ab	33.7±1.7b
Caffeicacid	0.2±0.03a	0.1±0.06a	0.1±0.06a	0.2±0.02a	0.06±0.06a	0.1±0.06a	0.18±0.01a	0.14±0.07a
Ferulic acid†	0.0±0.00a	0.00±0.00a	0.00±0.00a	0.00±0.00a	0.06±0.06a	0.00±0.00a	0.17±0.00a	0.19±0.01a
Quercetin-3-*O*-Galactoside†	0.2±0.15a	0.16±0.16a	0.45±0.02a	0.16±0.16a	0.31±0.16a	0.15±0.15a	0.47±0.03a	0.48±0.03a
Quercetin-3-*O*-Glucoside†	0.3±0.30a	0.30±0.30a	0.89±0.03a	0.31±0.31a	0.61±0.31a	0.30±0.30a	0.89±0.03a	0.91±0.02a
Quercetin-3-*O*-Rhamnoside	0.3±0.02a	0.24±0.00a	0.28±0.01a	0.22±0.02a	0.24±0.02a	0.24±0.02a	0.24±0.01a	0.24±0.01a
Catechin	8.6±0.5ab	6.04±0.42a	6.8±1.67ab	6.20±0.19b	7.10±0.68b	4.7±0.67ab	4.62±0.44b	4.65±1.01b
Epicatechin	39.9±0.5a	26.3±1.66b	26.5±2.86b	23.4±0.3bc	24.1±1.8bc	15.3±2.56c	17.3±1.47c	12.7±0.34c

* Means ± standard error (n=3)

† Non-parametric methods were used when normality of the error terms could not be achieved with transformed values.

Means sharing same letter within a row are not significantly different [Tukey's Studentized Range test ($P < 0.05$)].

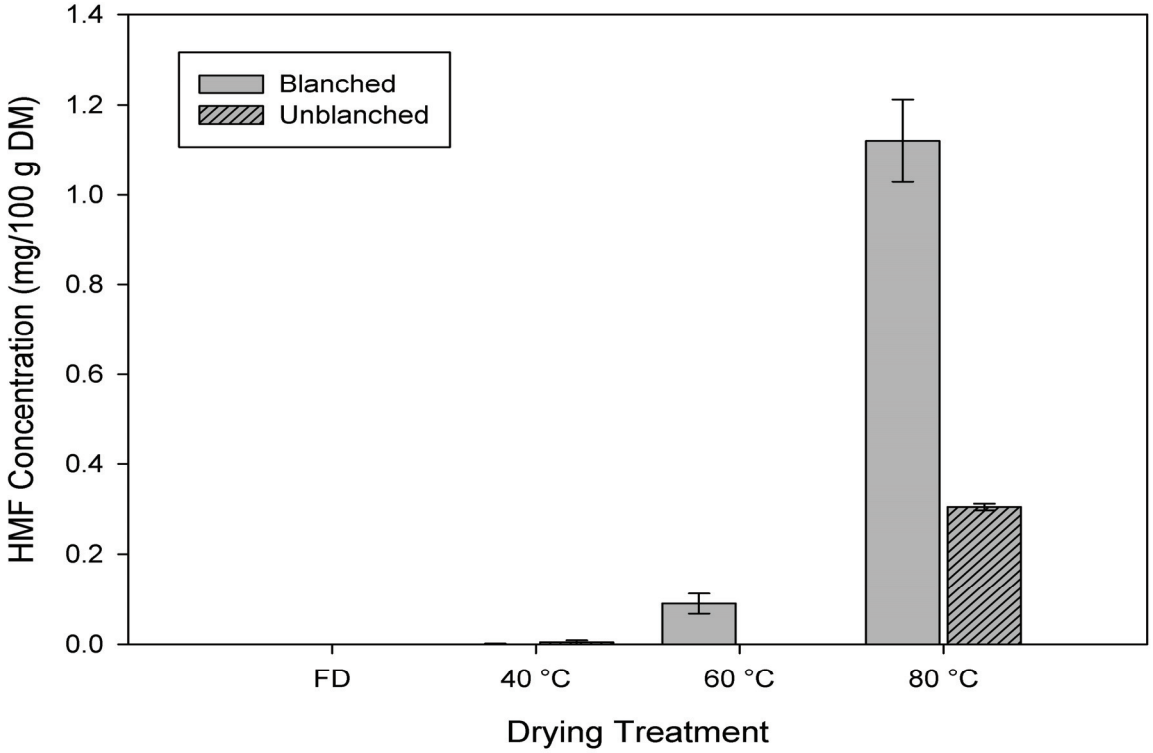

Figure 6.1 HMF Concentration of apple slices after dehydration at different temperatures. FD, freeze dried; DM, dry matter. Error bars represent standard error.

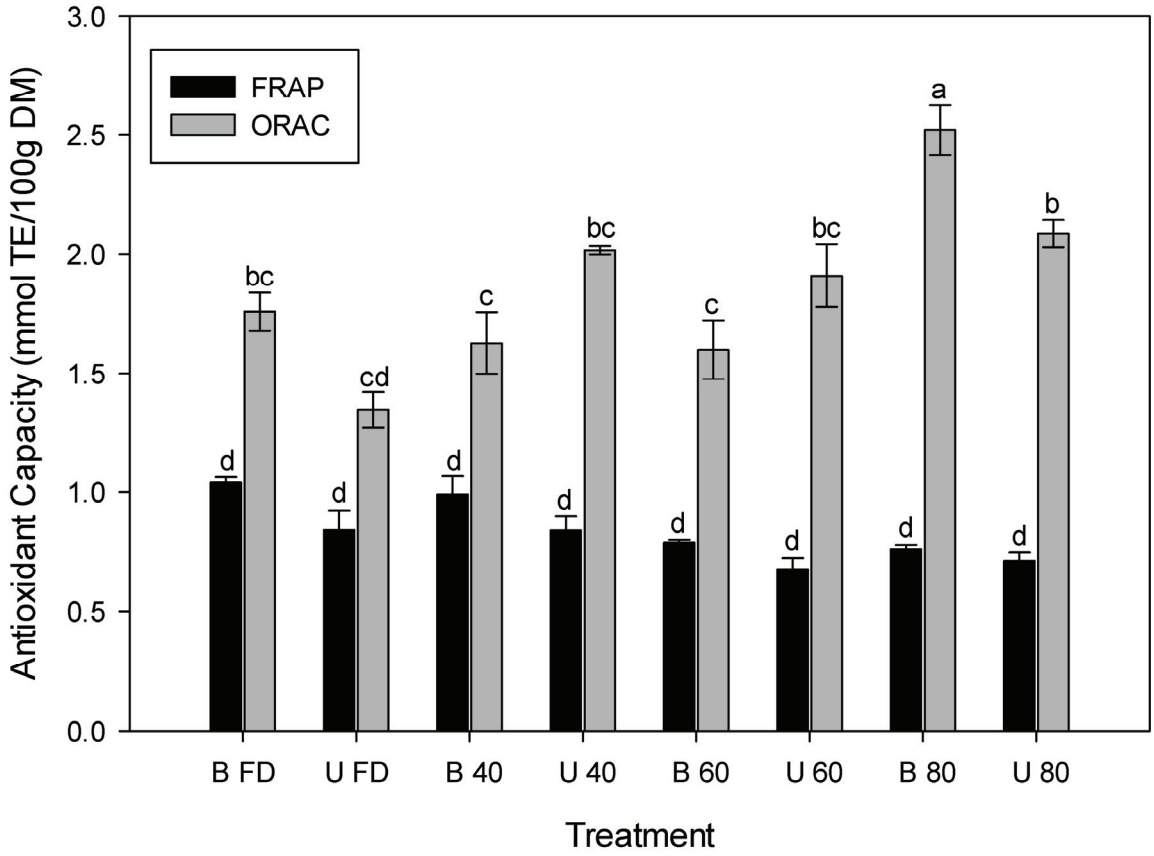

Figure 6.2 Antioxidant capacity measured by FRAP and ORAC assays of apple slices after processing at different temperatures. Means sharing the same letter are not significantly different [Tukey's Studentized Range test ($P < 0.05$)]. Error bars represent standard error. B, blanched; U, unblanched

6.3.2 Real-time Study Results

Within the first 2 hours of the drying process, significant color changes in hue and light intensity occurred in both the core and flesh of 'Gravenstein' apple slices. A decreasing trend in hue angle and color intensity was observed in the core tissue after 3.5 hours, becoming significant at 6.5 hours (Figure 6. 4). After 1 hour, color intensity of the core was significantly lower than that of the flesh.

Significant decreases in chlorogenic acid and epicatechin were also observed within the first half hour and continued to decrease during the entire process (Figure 6.4). Pearson correlation coefficients were calculated over the entire drying process (Table

6.2), for the first 2.5 hours (Table 6.3), and for the last 4 hours (Table 6.4) of the drying process. Epicatechin correlated with changes in hue of the apple slice flesh ($r = 0.4000$, $p = 0.0285$) over the entire drying process. Chlorogenic acid correlated significantly with intensity in both the core ($r = -0.6241$, $p = 0.030$) and flesh ($r = -0.8755$, $p < 0.001$) of the apple slices during the last 4 hours of the drying process.

HMF developed significantly in the apple slice after 4 hours (Figure 6.5) and correlated significantly with hue in the apple slice core ($r = -0.7908$, $p = 0.002$) during the last 3 hours of the drying process. During the first 2.5 hours, HMF development did not significantly correlate with hue and intensity. Whiteness index correlated with antioxidant capacity in both the core and flesh.

The antioxidant capacity, as measured by FRAP, followed a decreasing trend becoming significant after 1.5 hours of drying (Figure 6.6). No significant correlations between antioxidant capacity and HMF could be found.

Table 6.2 Pearson correlation coefficients and their p-values between color measurements and bioactive parameters over the entire drying process

		Hue Angle		Chroma		Intensity		Whiteness Index	
		Core	Flesh	Core	Flesh	Core	Flesh	Core	Flesh
Antioxidant Capacity (FRAP)	r	0.3054	0.2989	-0.2291	-0.2741	0.3315	0.1543	0.2791	0.2811
	p	0.129	0.138	0.260	0.175	0.098	0.452	0.167	0.164
Phenolics									
Epicatechin	r	0.2618	0.4000	-0.1251	-0.4164	-0.1703	-0.2318	0.0017	0.2077
	p	0.162	0.0285	0.510	0.022	0.368	0.2178	0.993	0.271
Catechin	r	0.0430	0.1624	0.1025	-0.1809	-0.3737	-0.4245	-0.2265	-0.0649
	p	0.821	0.391	0.590	0.339	0.0419	0.0194	0.229	0.733
Chlorogenic Acid	r	-0.0227	0.1144	0.2076	-0.1157	-0.3604	-0.3151	-0.2851	-0.0633
	p	0.905	0.547	0.271	0.543	0.050	0.090	0.127	0.7396
HMF	r	-0.5745	-0.4041	0.6506	0.4586	-0.3485	-0.0028	-0.5526	-0.3594
	p	0.001	0.0268	<0.001	0.011	0.059	0.988	0.002	0.051

r = Pearson correlation coefficient

Table 6.3 Pearson correlation coefficients and their p-values between color measurements and bioactive parameters during the first 2.5 hours of the drying process

		Hue Angle		Chroma		Intensity		Whiteness Index	
		Core	Flesh	Core	Flesh	Core	Flesh	Core	Flesh
Antioxidant Capacity	r	0.5447	0.4910	-0.6071	-0.5286	0.6718	0.4659	0.6716	0.6110
	p	0.036	0.063	0.016	0.043	0.006	0.080	0.006	0.016
Phenolics									
Epicatechin	r	-0.0608	0.2132	0.2709	-0.2016	-0.3691	-0.1856	-0.3317	0.0346
	p	0.811	0.396	0.277	0.423	0.132	0.461	0.179	0.892
Catechin	r	-0.2885	-0.0316	0.5157	0.0463	-0.5945	-0.3900	-0.5782	-0.2402
	p	0.246	0.901	0.029	0.855	0.009	0.110	0.012	0.337
Chlorogenic Acid	r	-0.1955	0.0339	0.4035	-0.0205	-0.4042	-0.1854	-0.4219	-0.0886
	p	0.437	0.894	0.097	0.936	0.096	0.462	0.081	0.727
HMF	r	-0.1968	-0.2286	0.2235	0.2805	0.0164	0.2504	-0.1150	-0.0691
	p	0.434	0.362	0.373	0.260	0.949	0.316	0.650	0.785

r = Pearson correlation coefficient

Table 6.4 Pearson correlation coefficients and their p-values between color measurements and bioactive parameters during the last 4 hours of the drying process

		Hue Angle		Chroma		Intensity		Whiteness Index	
		Core	Flesh	Core	Flesh	Core	Flesh	Core	Flesh
Antioxidant Capacity	r	-0.5143	-0.9196	0.3528	0.9025	-0.1162	-0.6665	-0.2530	-0.9024
	p	0.106	<0.001	0.287	<0.001	0.734	0.025	0.453	<0.001
Phenolics									
Epicatechin	r	0.1300	-0.2350	0.1100	0.1068	-0.1910	-0.3759	-0.1479	-0.2635
	p	0.687	0.462	0.734	0.741	0.552	0.229	0.647	0.408
Catechin	r	-0.0864	-0.4546	0.2957	0.2975	-0.3215	-0.5977	-0.3113	-0.4998
	p	0.789	0.138	0.351	0.348	0.308	0.040	0.325	0.098
Chlorogenic Acid	r	-0.5156	-0.5702	0.6772	0.3964	-0.6241	-0.8755	-0.6626	-0.7057
	p	0.086	0.053	0.016	0.202	0.030	<0.001	0.019	0.010
HMF	r	-0.7908	-0.2471	0.6447	0.2274	-0.4949	-0.4637	-0.5860	-0.3831
	p	0.002	0.439	0.024	0.477	0.102	0.129	0.045	0.219

r = Pearson correlation coefficient

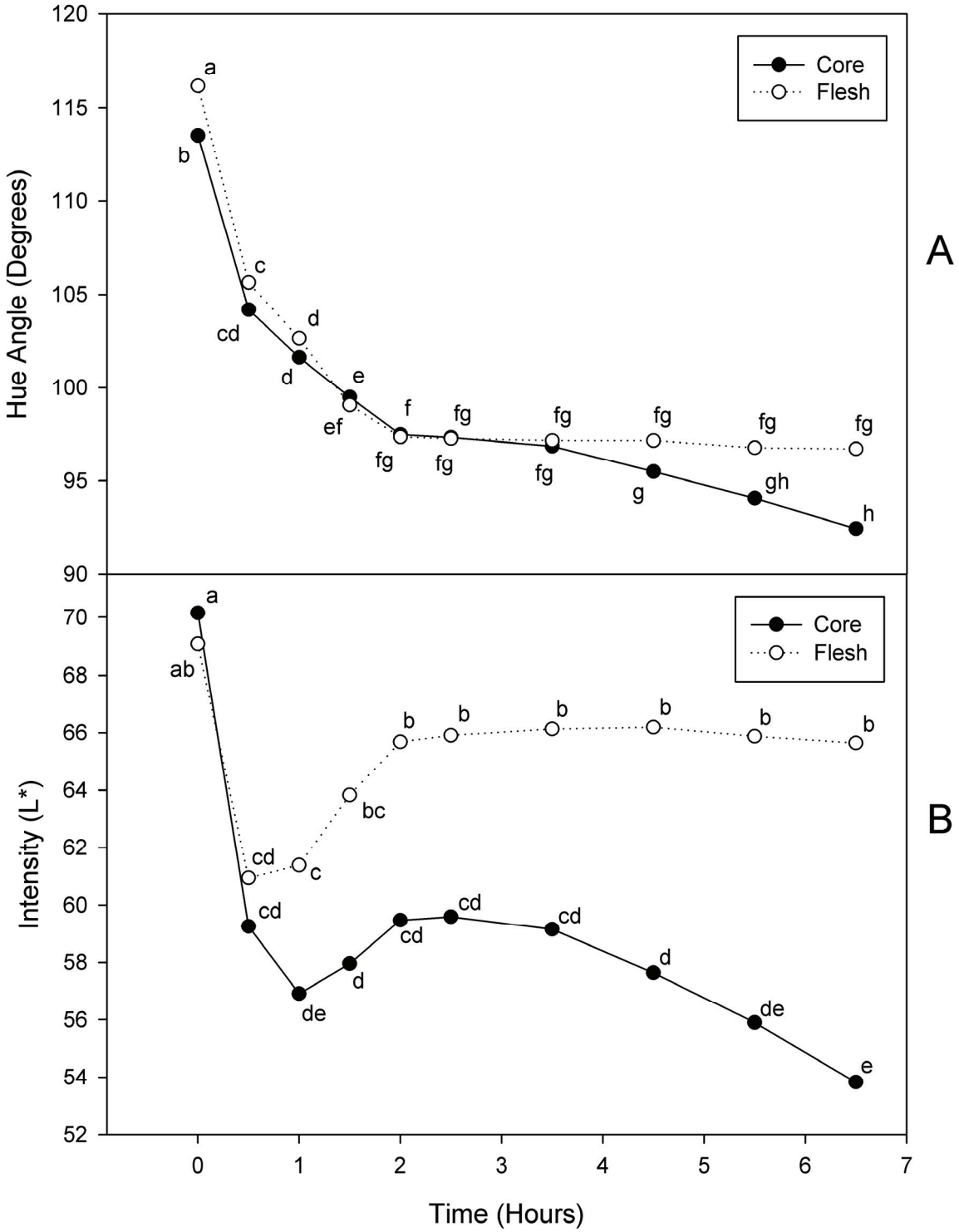

Figure 6.3 Changes in hue angle (A) and light intensity (B) within the core and flesh of apple slices during dehydration at 80 °C.

Means sharing same letter are not significantly different [Tukey's Studentized Range test ($P < 0.05$)].

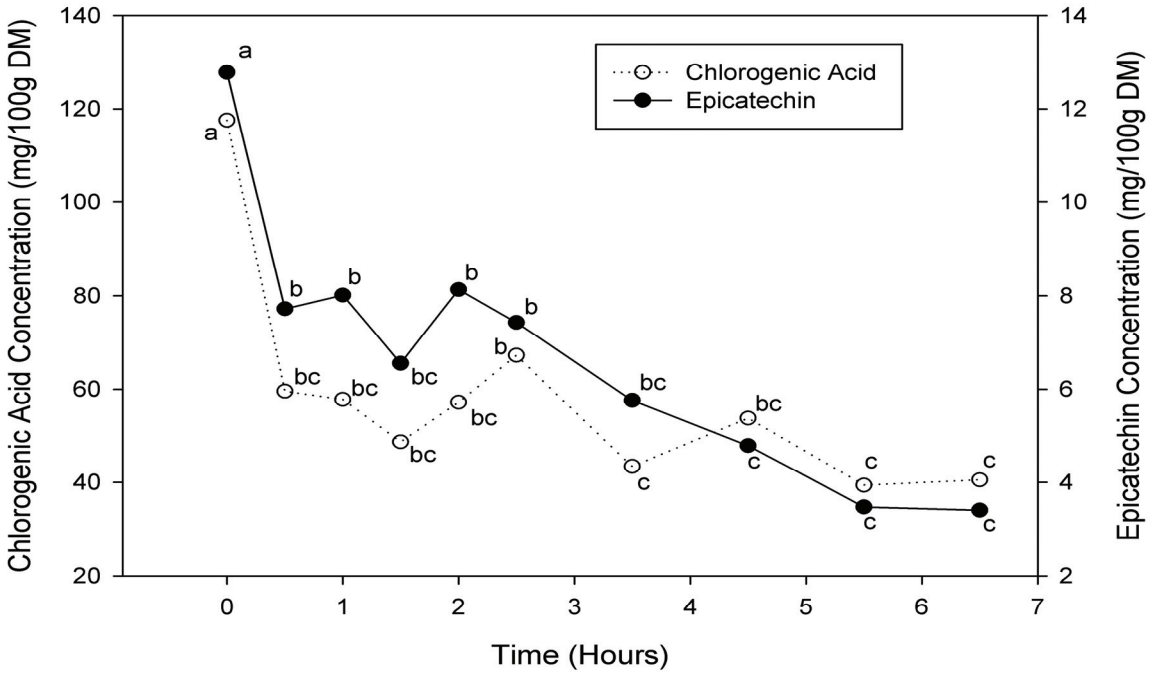

Figure 6.4 Time series degradation of chlorogenic acid and epicatechin during apple slice thermal processing at 80 °C.

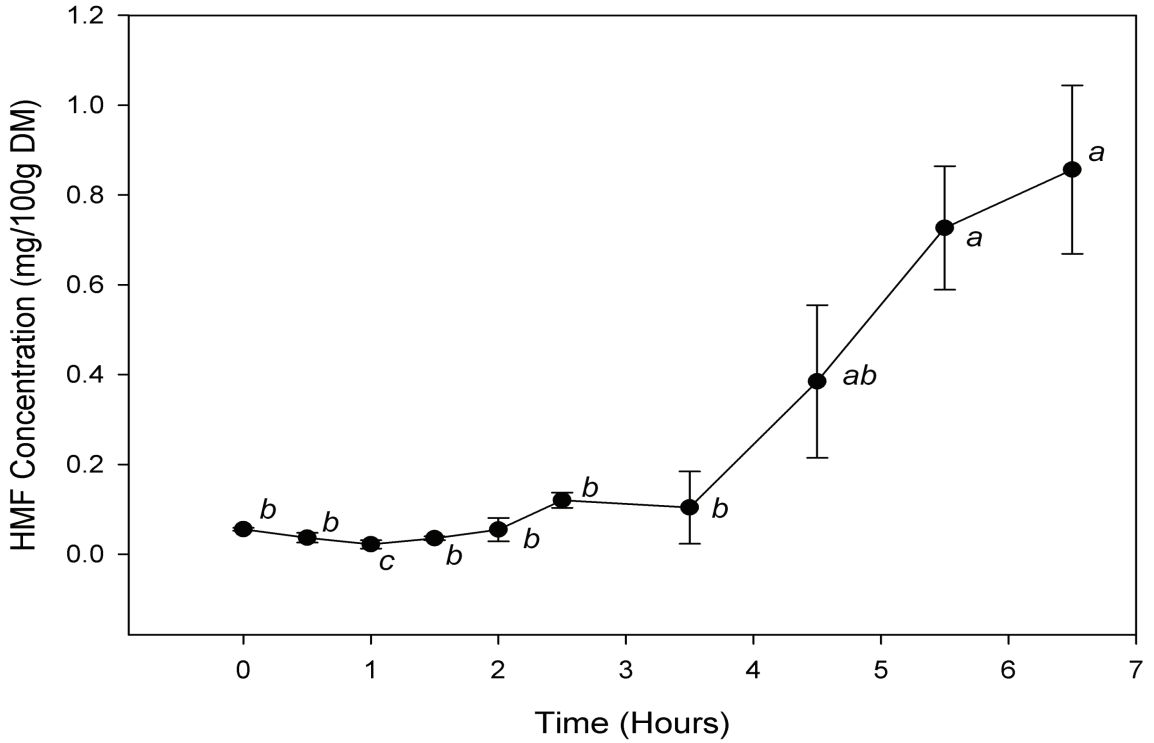

Figure 6.5 Time series development of HMF during apple slice thermal processing at 80 °C.

Means sharing same letter are not significantly different [Tukey's Studentized Range test ($P < 0.05$)]. Error bars represent standard error.

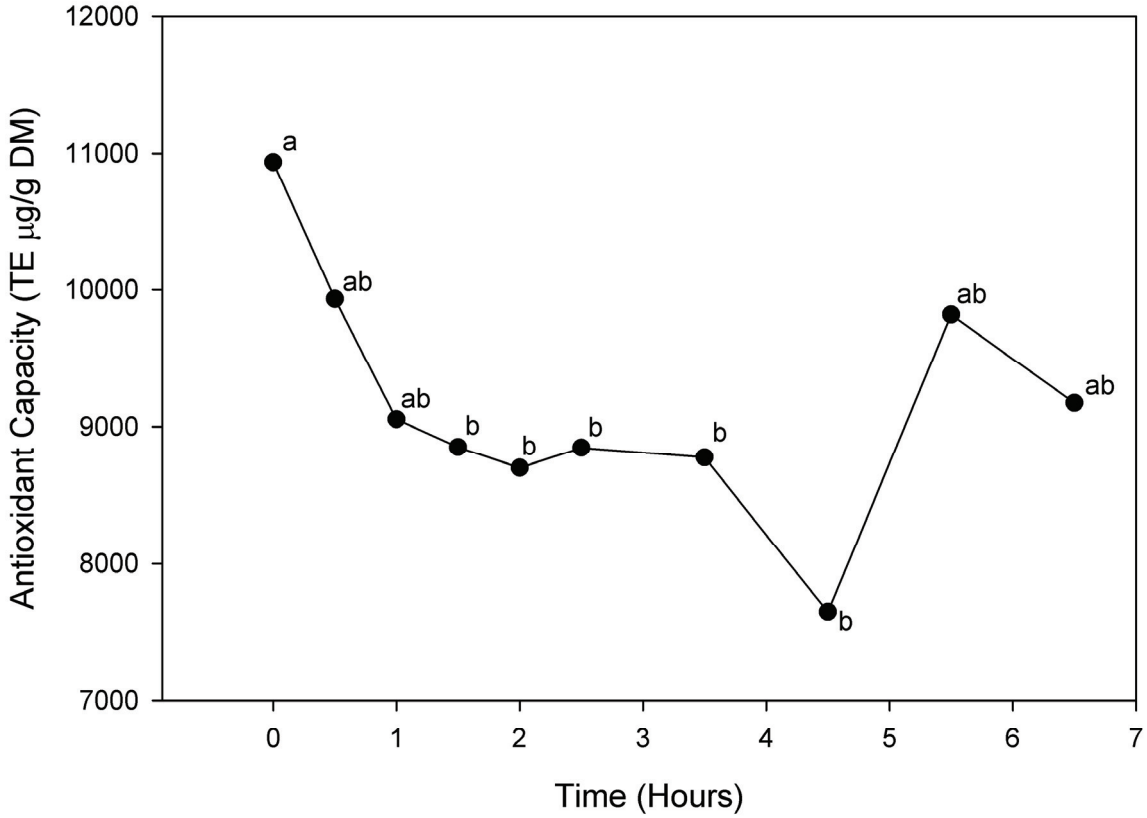

Figure 6.6 FRAP measurements of antioxidant capacity changes of apple slices during thermal processing at 80 °C. TE; Trolox equivalents. Means sharing the same letter are not significantly different [Tukey's Studentized Range test ($P < 0.05$)].

6.4 Discussion

Epicatechin correlated well with changes in hue and chroma as measured from the computer vision system over the entire drying process. Catechin was inversely correlated with the color intensity in the core and flesh, while chlorogenic acid was inversely correlated with the color intensity in the flesh during the entire drying process. HMF correlated with hue, chroma, and Whiteness Index of core and flesh over the entire drying process. The above correlations were more pronounced in the core when compared to that of the flesh. Therefore, color changes in the core of the apple likely indicate the presence of Maillard reactions and HMF development. When the data was split to analyze the first

(first 2.5 hours) and second (last 4 hours) periods of drying, certain coefficients between color measurements and phenolics were falsely significant due to fewer measurements resulting in type I experimental error.

The decrease in total phenolics for the unblanched treatment was greater overall than for the blanched treatment indicating that the blanching treatment deactivates the PPO enzymes in apple slices (Severini et al. 2003). Therefore, blanching could be used during commercial thermal processing to prevent further loss of these polyphenolic compounds. An interesting point is that HMF concentration increased significantly at 80 °C, but was higher in blanched than unblanched samples. This finding suggests that blanching promotes HMF development, while reducing the degradation of phenolic compounds.

HMF did not develop in the unblanched apple slices at either the 40 °C or 60 °C drying temperatures and therefore it was not necessary to perform a time-series experiment to monitor the development of HMF at these temperatures. From a food safety standpoint, the lack of HMF development at the lower temperatures indicates that HMF would not be a health issue for apples processed at 60 °C or less. The use of low drying temperatures below 60 °C to reduce HMF concentration in combination with blanching to preserve phenolic compounds is recommended.

Thermal processing of apple slices has been shown to degrade phenolic compounds, such as chlorogenic acid and epicatechin, as well as promote the development of HMF at higher processing temperatures. Relationships between phenolic compounds, antioxidants and color changes, as well as HMF and color changes were characterized and used as the basis for computer-vision measurements of these

parameters. During the first 2.5 hours, the color intensity in the flesh was significantly higher than the intensity in the core, while the hue values were approximately the same. The explanation for this phenomenon could be due to the distribution of chlorogenic acid within the apple fruit. Awad et al. (2000) characterized the distribution of chlorogenic acid and other phenolics and found more chlorogenic acid in the core than in the flesh of 'Jonagold' and 'Elstar' apple varieties. In 'Golden Delicious' apples, chlorogenic acid was also higher in the core than in the flesh (Mayr et al. 1995). The lower intensity of the core could be indicative of this trend as a higher concentration of chlorogenic acid would appear as a darker brown color. The development of HMF steadily increased after 4.5 hours of drying at 80 °C. During the last 4.5 hours of drying, changes in the core hue correlated with HMF suggesting that HMF development may begin in the core of the apple slice. The distribution of reducing sugars in apple tissue has not been reported, but the concentration of reducing sugars was found to be much higher in the core of pears than in the flesh (Martin 1936). Román-Leshkov et al. (2006) have documented a method to convert fructose into HMF. It is therefore recommended that further research be conducted to determine the sugar profiles of apples to determine if this could explain the color change.

6.5 Conclusion

Though it is well known that HMF develops under higher temperature conditions, the Quinté apple slices developed HMF when dried at 80 °C, but not at 40 °C or 60 °C. Blanching, by dipping apple slices in $CaCl_2$ (1.6% v/v), promoted HMF development and therefore may not be a desirable technique if HMF development is to be inhibited.

Color changes were measurable in the flesh and core of the apple slice using the computer-vision system. Significant hue and intensity changes occurred between the core and flesh and also over time. The color changes in the core after 4.5 hours were closely correlated with changes in HMF concentration. Further verification is necessary to determine if this color change is due to HMF development.

CHAPTER 7 CONCLUSIONS

7.1 OBJECTIVE OF THE STUDY

The consumer demand for quality food provided reason for developing non-contact measurements during the drying of fruits. Currently, disruptive contact measurements must be taken to assess food quality, which has the potential to cause food contamination and destruction. Computer-vision is a strong candidate in reducing human error and food contamination and has been implemented in many areas of food inspection. The objective was to extend the use of computer-vision for food quality measurements during apple slice drying.

The approach for preparing the computer-vision cameras for objective measurements involved determining the specific camera settings such as black level, gain, and saturation and white balancing to optimize lighting and color measurements. Non-uniform illumination and lens distortions were corrected to ensure maximum use of the photographic region. Correlations were determined between computer-vision measurements and physical measurements (area, thickness, color) using inert objects to obtain accurate measurements of these geometric and colorimetric properties.

The information collected from objective 1 was used to assess the ability of the computer-vision system to measure volume and texture characteristics (peak force, initial slope and work done according to stress-strain curves) as well as the end of drying time. Whether camera color measurements correlated with polyphenolic degradation and hydroxymethylfurfural development was investigated and antioxidant capacity of apple slices after drying treatments at different temperatures was assessed.

7.2 General Discussion

In the camera preparation study, a suitable method of correcting non-uniform illumination and lens distortions was found so that the entire imaging region could be used. A procedure was developed to correct color problems from the type of lighting so that any type of light can be used. The brightness, gain, saturation, and color balance settings were also determined for this particular system. With the given spatial resolution of most cameras, the computer-vision system proved to be very accurate at measuring geometric properties of objects. While the computer-vision system had the ability to measure the color of many parts of an object at one time, the accuracy was much lower than a colorimeter, though from an inspection standpoint, the accuracy may still be acceptable pending further investigation of industrial practices. The relationships between actual geometric and colorimetric properties and image interpretations of objects have been determined for this particular computer-vision system.

In the volume and texture study, the uniformity image texture feature was found to be a good indicator of the end of drying process, while apple slice volume was not effective because of porosity development. As the apple decreased in size and continued to bend the image representation of the apple slice became more uniform as more pixels were being added to the background. The desorption isotherm which relates the moisture content with the water activity at room temperature was determined. Image texture analysis results did not correlate with textural features.

Upon examining the temperature sensitivity of the phenolics compounds within the apple slices, it was observed that chlorogenic acid, catechin, and epicatechin were more preferred substrates for PPO activity. Blanching did preserve the phenolics

compounds. Hydroxymenthylfurfural (HMF) also developed in the unblanched slices at 80 °C, but not at 40 °C or 60 °C, where in the blanched slices HMF developed at 60 °C and 80 °C. HMF was significantly higher at 60 °C and 80 °C in the blanched apple slices suggesting that blanching may promote HMF development. The computer-vision system was able to detect color changes in multiple places that correlated well with HMF development and phenolic concentrations.

7.3 Recommendations and Future Research

Computer-vision and imaging technologies are always changing. To further increase the spatial calibration process, many of the inert objects used to calibrate the area can be combined into a single object of multiple features, colors, and sizes. It is recommended that these objects be combined for industry so that the spatial and colorimetric calibrations can be done quickly and consistently. High-end cameras can be used to address the low accuracy problem for the color measurements.

Image texture analysis has much greater potential for identifying many pattern changes in drying processes. Though correlations between image texture features and physical texture features could not be found, it is recommended for future research that a more extensive feature set and analysis techniques be used to investigate other possible links.

Degradation of useful polyphenolic compounds is not desired. The desirability of HMF development in apple slices is not known, and therefore presents an area of future research. Based on the computer-vision results, it is recommended that the distribution of reducing sugars within the apple slice be explored along with HMF development to

determine if computer-vision was able to detect the presence of HMF based on the vision parameters.

In conclusion, computer-vision is capable of non-contact measurements of many food quality attributes. At this stage, the computer-vision system must often be custom designed and configured for a particular task. Further development will increase the ability for such systems to be deployed and provide centralized information collection and increase the management and efficiency of the food inspection process.

REFERENCES

Abbott, J. A., Saftner, R. A., Gross, K. C., Vinyard, B. T. and Janick, J. 2004. Consumer evaluation and quality measurement of fresh-cut slices of 'fuji' 'golden delicious' 'goldrush' and 'granny smith' apples. Postharvest Biol. Tec. **33**:127-140.

American Society for Testing and Materials. 2004a. C 914-95 Standard test method for bulk density and volume of solid refractories by wax immersion.

American Society for Testing and Materials. 2004b. E 313 Standard Practice for Calculating Yellowness and Whiteness Indices from Instrumentally Measured Color Coordinates.

Association of Official Agricultural Chemists. 1998. AOAC official method 980.23 hydroxymethylfurfural in honey.

Awad, A. M., de Jager, A. and van Westing, L. M. 2000. Flavonoid and chlorogenic acid levels in apple fruit: characterisation of variation. Sci. Hortic-Amsterdam. **83**:249-263.

Benzie, I. F., Strain and J.J. 1996. The ferric reducing ability of plasma (FRAP) as a measure of "antioxidant power": The FRAP assay. Anal. Biochem. **239**:70-76.

Blasco, J., Aleixos, N. and Moltó, E. 2003. Machine vision system for automatic quality grading of fruit. Biosystems Eng. **85**:415-423.

Brosnan, T. and Sun, D.-W. 2004. Improving quality inspection of food products by computer-vision-a review. J. Food Eng. **61**:3-16.

Brown, D. C. 1966. Decentering distortion of lenses. Photogram. Eng. **32**:444-462.

Chen, X.D. 2008. Food drying fundamentals *in* Drying Technologies in Food Processing. pp. 1-54 (Chen, X.D.ed.). Blackwell Publishing, U.K.

Clausi, D. A. 2002. An analysis of co-occurrence texture statistics as a function of grey level quantization. Can. J. Remote Sensing. **28**:45-62.

Commission Internationale d'Éclairage. 2007. CIE Colorimetry - Part 4: 1976 L*a*b* Color Space. [Online]. Avaliable: http://www.cie.co.at/index.php/index.php?i_ca_id=485 [October 17, 2009].

DeFeudis, F.V. and Drieu, K. 2000. Ginkgo biloba extract (EGb 761) and CNS functions: Basic studies and clinical applications. Curr. Drug Targets. **1**:25-58.

Deltel, G., Gagné, C., Lemieux, A., Levert, M., Liu, X. and Najjar, L. 2001. Automated measurement of cylinder volume by vision. [Online]. Available: http://vision.gel.ulaval.ca/~alemieux/pubs/fringe_01_Uni_Laval.pdf [October 12, 2009].

Fernández, L., Castillero and C., Aguilera, J. M. 2005. An application of image analysis to dehydration of apple discs. J. Food Eng. **67**:185-193.

Fillion, L. and Kilcast, D. 2002. Consumer perception of crispness and crunchiness in fruits and vegetables. Food Qual. Prefer. **13**:23-29.

Francis, F. J. 1995. Quality as influenced by color. Food Qual. Prefer. **6**:149-155.

Garayo, J. and Moreira, R. 2002. Vacuum frying of potato chips. J. Food Eng. **55**:181-191.

Gil, M. I., Tomás-Barberán, F. A., Hess-Pierce, B., Holcroft, D. M. and Kader, A. A. 2000. Antioxidant activity of pomegranate juice and its relationship with phenolic composition and processing. J. Agric. Food Chem. **48**:4581-4589.

Gökman, V. and Şenyuva, H. 2006. Improved method for the determination of hydroxymethylfurfural in baby foods using liquid chromatography-mass spectrometry. J. Agric. Food Chem. **54**:2845-2849.

Gunasekaran, S. 2000. Nondestructive food evaluation: techniques to analyze properties and quality. Marcel Dekker., New York, NY.

Harel, E., Mayer, A. M. and Shain, Y. 1964. Catechol oxidases from apples, their properties, subcellular location and inhibition. Physiol. Plantarum **12**:921-930.

Harlick, R. M. 1979. Statistical and structural approaches to texture. Proc. IEEE. **67**:786-804.

Henríquez, C., Almonacid, S., Chiffelle, I., Valenzuela, T., Araya, M., Cabezas, L., Simpson, R. and Speisky, H. 2010. Determination of antioxidant capacity, total phenolic content and mineral composition of different fruit tissue of five apple cultivars grown in Chile. Chil. J. Agr. Res. **70**:523-536.

Huber, G.M. and Rupasinghe, H.P.V. 2009. Phenolic profiles and antioxidant properties of apple skin extracts. J. Food Sci. **74**:693-700.

Ibarz, A., Pagán, S. and Garza, S. 1999. Kinetic models for colour changes in pear puree during heating at relatively high temperatures. J. Food Eng. **39**:415-422.

Jamradloedluk, J., Nathakaranakule, A., Soponronnarit, S. and Prachayawarakorn, S. 2007. Influences of drying medium and temperature on drying kinetics and quality attributes of durian chip. J. Food Eng. **78**:198-205.

Joseph, J.A., Shukitt-Hale, B. and Casadesus, G. 2005. Reversing the deleterious effects of aging on neuronal communication and behavior: beneficial properties of fruit polyphenolic compounds. Amer. J. Clin. Nutr. **81**:3135-3165.

Joshi, A. P. K., Rupasinghe, H. P. V., Pitts, N. L. and Khanizadeh, S. 2007. Biochemical characterization of enzymatic browning in selected apple genotypes. Can. J. Plant Sci. **87**:1067-1074.

Judd, D. B. 1963. Color in Business, Science, and Industry. Wiley, New York, NY.

Katsube, T., Tsurunaga, Y., Sugiyama, M., Furuno and T., Yamasaki, Y. 2009. Effect of air-drying temperature on antioxidant capacity and stability of polyphenolic compounds in mulberry (Morus alba L.) leaves. Food Chem. **113**:964-969.

Katz, E. E. and Labuza, T. P. 1981. Effect of water activity on the sensory crispness and mechanical deformation of snack food products. J. Food Sci. **46**:403-409.

Kawas, M. L. and Moreira, R. G. 2001. Effect of degree of starch gelatinization on quality attributes of fried tortilla chips. J. Food Sci. **66**:300-306.

Larrauri, J. A., Rupérez, P. and Saura-Calixto, F. 1997. Effect of drying temperature on the stability of polyphenols and antioxidant activity of red grape pomace peels. J. Agric. Food Chem. **45**:1390-1393.

Lee, D.-J. 2002. Patent No. 6369401. United States of America.

Lee, D. J., Xu, X., Eifert, J. and Zhan, P. 2006. Area and volume measurements of objects with irregular shapes using multiple silhouettes. Opt. Eng. **45**:1-11.

León, K., Mery, D., Pedreschi, F. and León, J. 2006. Color measurement in L*a*b* units from RGB digital images. Food Res. Int. **39**:1084-1091.

Levine, L., Huang, V. T. and Saguy, I. 1990. Use of computer-vision for real time estimation of volume increase during microwave baking. Cereal Chem. **67**:104-105.

Lewicki, P. P. 2004. Water as the determinant of food engineering properties-A review. J. Food Eng. **61**:483-495.

Lozano, J. E., Rotstein, E. and Urbicain, M. J. 1980. Total porosity and open-pore porosity in the drying of fruits. J. Food Sci. **45**:1403-1407.

Lu, W. and Sun, D.-W. 2000. Computer-vision systems for rapid quality inspection of agricultural and food products. Technology Innovation and Sustainable Agriculture p. 201-206. International Conference on Engineering and Technological Sciences.

Luo, Y. and Barbosa, G., 1997. Enzymatic browning and its inhibition in new apple cultivars slices using 4-hexylresorcinol in combination with ascorbic acid. Food Sci. Technol. Int. **3**:195–201.

Madrau, M. A., Piscopo, A., Sanguinetti, A. M., Del Caro, A., Poiana, M., Romeo, F. V. and Piga, A. 2009. Effect of drying temperature on polyphenolic content and antioxidant activity of apricots. Eur. Food Res. Technol. **228**:441-448.

Marks, B. P. 2006. Thermal Processing of Foods: Principles and Applications. In Y. H. Edt. Hui, Handbook of Food Science, Technology, and Engineering (Vol. III, pp. 107-1 to 107-14). Taylor & Francis. Boca Raton, Florida.

Martin, W. E. 1936. Distribution of certain sugars in bosc pears. Plant Physiol. **11**:139-147.

Martynenko, A. I. 2006. Computer-vision system for control of drying processes. Dry. Technol. **24**:879-888.

Martynenko, A. I. 2008. Porosity evaluation of ginseng roots from real-time imaging and mass measurements. Food and Bioprocess Technology. **4**:417-428.

Mayr, U., Treutter, D., Santos-Buelga, C., Bauer, H. and Feucht, W. 1995. Growth and metabolism developmental changes in the phenol concentrations of 'Golden Delicious' apple fruits and leaves. Phytochemistry. **38**:1151-1155.

McEvily, A.J., Iyengar, R. and Otwell, W.S., 1992. Inhibition of enzymatic browning in foods and beverages. Crit. Rev. Food Sci. **32**:253–273.

Mendoza, F., Dejmek, P. and Aguilera, J. M. 2007. Color and image texture analysis in classification of commercial potato chips. Food Res. Int. **40**:1146-1154.

Mittal, G. S. 1996. Computerized control systems in the food industry. Marcel Dekker., New York, NY.

Nishino, K., Kato, H. and Torii, K. 2000. Stereo imaging for simultaneous measurement of size and velocity of particles in dispersed two-phase flow. Meas. Sci. Technol. **11**:633-645.

Omura, H., Jahan, N., Shinohara, K. and Murakami, Y. 1983. Formation of Mutagens by the Maillard Reaction. Pages 537-563 *in* The maillard reaction in foods and nutrition. American Chemical Society, Washington, DC.

Pedreschi, F., León, J., Mery, D. and Moyano, P. 2006. Development of a computer-vision system to measure the color of potato chips. Food Res. Int. **39**:1092-1098.

Pereira, A. C., Reis, M. S. and Saraiva, P. M. 2009. Quality control of food products using image analysis and multivariate statistical tools. Ind. Eng. Chem. Res. **48**:988-998.

Piga, A., Del Caro, A. and Corda, G. 2003. From plums to prunes: influence of drying parameters on polyphenols and antioxidant activity. J. Agric. Food Chem. **51**:3675-3681.

Pintavirooj, C. and Sangworasil, M. 2002. 3D-Shape reconstruction based on radon transform with applications in volume measurement. Winter School of Computer Graphics (WSCG). (pp. 1-4).

Pizzocardo, F., Torreggiani, D. and Gilardi, G. 1993. Inhibition of apply polyphenoloxidase (PPO) by ascorbic acid, citric acid and sodium chloride. J. Food Process. Pres. **17**:21-30.

Prior, R. L., Cao, G., Martin, A., Sofic, E., McEwen, J., O'Brien, C., Lischner, N., Ehlenfeldt, M., Kalt, W., Krewer, G. and Mainland, C. M. 1998. Antioxidant capacity as influenced by total phenolic and anthocyanin content, maturity, and variety of vaccinium species. J. Agric. Food Chem. **46**:2686-2693.

Prothon, F. and Ahrné, L. M. 2004. Application of the Guggenheim, Anderson and De Boer model to correlate water activity and moisture content during osmotic dehydration of apples. J. Food Eng. **61**:467-470.

Rada-Mendoza, M., Sanz, M., Olano, A. and Villamiel, M. 2004. Formation of hydroxymethylfurfural and furosine during the storage of jams and fruit-based infant foods. Food Chem. **85**:605-609.

Raynal, J., Moutounet, M. and Souquet, J. M. 1989. Intervention of phenolic compounds in plum technology. 1. Changes during drying. J. Agric. Food Chem. **37**:1046-1050.

Resnik, S. and Chirife, J. 1979. Effect of moisture content and temperature on some aspects of nonenzymatic browning in dehydrated apple. J. Food Sci. **44**:601-605.

Román-Leshkov, Y., Chheda, J. N. and Dumesic, J. A. 2006. Phase modifiers promote efficient production of hydroxymethylfurfural from fructose. Science. **312**:1933-1937

Roudaut, G., Dacremont, C., Vallès Pàmies, B., Colas, B. and Le Meste, M. 2002. Crispness: a critical review on sensory and material science approaches. Trends Food Sci. Tech. **13**:217-227.

Rosatella, A. A., Simeonov, S. P., Fradea, R. M. F. and Alfonso, C. A. M. 2011. 5-Hydroxymethylfurfural (HMF) as a building block platform: Biological properties, synthesis and synthetic applications. Green Chem. **13**:754-793.

Ruff, B. P., Marchant, J. A. and Frost, A. R. 1995. Fish sizing and monitoring using a stereo image analysis system applied to fish farming. Aquacult. Eng. **14**:155-173.

Rupasinghe, H. P. V., Wang, L., Huber, G. M. and Pitts, N. L. 2008. Effect of baking on dietary fibre and phenolics of muffins incorporated with apple skin powder. Food Chem. **107**:1217-1224.

Russ, J. 1992. Segmentation and Thresholding. Pages 225-275 *in* The Image Processing Handbook. CRC Press. Boca Raton, Florida.

Russ, J. C. 2005. The need for stereology. Pages 1-2 *in* Image Analysis of Food Microstructure. CRC Press LLC. Boca Raton, Florida.

Sanz, M., del Castillo, M., Corzo, N. and Olano, A. 2001. Formation of Amadori compounds in dehydrated fruits. J. Agric. Food Chem. **49**:5228-5231.

Sato, M., Bagchi, D., Tosaki, A. and Das, D.K. 2001. Grape seed proanthocyanidin reduces cardiomyocyte apoptosis by inhibiting ischemia/reperfusion-induced activation of JNK-1 and C-JUN. Free Radic. Biol. Med. **31**:729-737.

Segnini, S., Dejmek, P. and Öste, R. 1999a. A low cost video technique for color measurement of potato chips. Lebensm. Wiss. Technol. **32**:216-222.

Segnini, S., Dejmek, P. and Öste, R. 1999b. Relationship between instrumental and sensory analysis of texture and color of potato chips. J. Texture Stud. **30**:677-690.

Sellappan, S., Akoh, C. C. and Krewer G. 2002. Phenolic compounds and antioxidant capacity of Georgia-grown blueberries and blackberries. J. Agric. Food Chem. **50**:2432-2438.

Severini, C., Baiano, A., De Pilli, T., Romaniello, R. and Derossi, A. 2003. Prevention of enzymatic browning in sliced potatoes by blanching in boiling saline solutions. Lebensm. Wiss. Technol. **36**:657-665.

Shah, S. and Aggarwal, J. K. 1996. Intrinsic parameter calibration procedure for a (high-distortion) fish-eye lens camera with distortion model and accuracy estimation. Pattern Recogn. **29**:1775-1788.

Sun, D.-W. 2004. Computer-vision-an objective, rapid and non-contact quality evaluation tool for the food industry. J. Food Eng. **61**:1-2.

Szczesniak, A. S. 2002. Texture is a sensory property. Food Qual. Prefer. **13**:215-225.

Teixidó, E., Santos, F., Puignou, L. and Galceran, M. 2006. Analysis of 5-hydroxymethylfurfural in foods by gas chromatography-mass spectometry. J. Chromatogr. A. **1135**:85-90.

Teixidó, E., Moyano, E., Santos, F. and Galceran, M. 2008. Liquid chromatography multi-stage mass spectrometry for the analysis of 5-hydroxymethylfurfural in foods. J. Chromatogr. A. **1185**:102-108.

Thompson, T. L. 1972. Temporary storage of high moisture shelled corn using continuous aeration. T. ASAE. **15**:333-337.

Tsao, R., Yang, R., Xie, S., Sockovie, E. and Khanizadeh, S. 2005. Which polyphenolic compounds contribute to the total antioxidant activities of apple? J. Agric. Food Chem. **53**:4989-4995.

Turkmen, N., Ferda, S. and Velioglu, Y. S. 2005. The effect of cooking methods on total phenolics and antioxidant activity of selected green vegetables. Analytical, Nutritional and Clinical Methods. **93**:713-718.

Ulbricht, R. J., Northup, S. J. and Thomas, J. A. 1984. A review of 5-hydroxymethylfurfural (HMF) in parenteral solutions. Fundam. Appl. Toxicol. **4**:843–853.

Vos, P. T. and Labuza, T. P. 1974. Technique for measurement of water activity in the high aw range. J. Agr. Food Chem. **22**:326-327.

Wang, H., Cao, G. and Prior, R. L. 1996. Total antioxidant capacity of fruits. J. Agric. Food Chem. **44**:701-705.

Webb, P. 2001. Volume and Density Determinations for Particle Technologists. [Online]. Available: http://www.micromeritics.com/Repository/Files/Volume_and_Density_determinations_for_Particle_Technologists_0.pdf [October 12, 2009].

Wilkinson, C., Dijksterhuis, G. B. and Minekus, M. 2000. From food structure to texture. Trends Food Sci. Tech. **11**:442-450.

Wojdylo, A., Oszmiański, J. and Laskowski, P. 2008. Polyphenolic compounds and antioxidant activity of new and old apple varieties. J. Agric. Food Chem. **56**:6520-6530.